Modelling gross primary production in semi-arid Inner Mongolia using MODIS imagery and eddy covariance data

Ranjeet John [a] , Jiquan Chen [a b] , Asko Noormets [c] , Xiangming
Xiao [d] , Jianye Xu [a] , Nan Lu [e] & Shiping Chen [b]

[a] Department of Environmental Sciences , University of Toledo ,
Toledo , OH , 43606 , USA

[b] Institute of Botany , Chinese Academy of Sciences , Beijing ,
100093 , People's Republic of China

[c] Department of Forestry and Environmental Resources and
Southern Global Change Program , North Carolina State
University , Raleigh , NC , 27695 , USA

[d] Center for Spatial Analysis, Stephenson Research and Technology
Center , University of Oklahoma , Norman , OK , 73019-5300 , USA

[e] Research Centre for Eco-Environmental Sciences , Chinese
Academy of Sciences , Beijing , 100085 , People's Republic of
China
Published online: 14 Jan 2013.

PLEASE SCROLL DOWN FOR ARTICLE

of information. Taylor and Francis shall not be liable for any losses, actions, claims, proceedings, demands, costs, expenses, damages, and other liabilities whatsoever or howsoever caused arising directly or indirectly in connection with, in relation to or arising out of the use of the Content.

This article may be used for research, teaching, and private study purposes. Any substantial or systematic reproduction, redistribution, reselling, loan, sub-licensing, systematic supply, or distribution in any form to anyone is expressly forbidden. Terms & Conditions of access and use can be found at http://www.tandfonline.com/page/terms-and-conditions

Taylor & Francis
Taylor & Francis Group

Modelling gross primary production in semi-arid Inner Mongolia using MODIS imagery and eddy covariance data

Ranjeet John[a]*, Jiquan Chen[a,b], Asko Noormets[c], Xiangming Xiao[d], Jianye Xu[a], Nan Lu[e], and Shiping Chen[b]

[a]*Department of Environmental Sciences, University of Toledo, Toledo, OH 43606, USA;* [b]*Institute of Botany, Chinese Academy of Sciences, Beijing 100093, People's Republic of China;* [c]*Department of Forestry and Environmental Resources and Southern Global Change Program, North Carolina State University, Raleigh, NC 27695, USA;* [d]*Center for Spatial Analysis, Stephenson Research and Technology Center, University of Oklahoma, Norman, OK 73019-5300, USA;* [e]*Research Centre for Eco-Environmental Sciences, Chinese Academy of Sciences, Beijing 100085, People's Republic of China*

We evaluate the modelling of carbon fluxes from eddy covariance (EC) tower observations in different water-limited land-cover/land-use (LCLU) and biome types in semi-arid Inner Mongolia, China. The vegetation photosynthesis model (VPM) and modified VPM (MVPM), driven by the enhanced vegetation index (EVI) and land-surface water index (LSWI), which were derived from the Moderate Resolution Imaging Spectroradiometer (MODIS) surface-reflectance product (MOD09A1), were used to model and validate the temporal changes in gross primary production (GPP) from the EC towers during the 2006 and 2007 growing seasons. The annual GPP predicted by the VPM model (GPP_{VPM}) was predicted reasonably well in 2006 and 2007 at the cropland (coefficient of determination, $R^2 = 0.67$ and 0.71, for 2006 and 2007, respectively) and typical steppe ($R^2 = 0.80$ and 0.73) sites. The predictive power of the VPM model varied in the desert steppe, which includes an irrigated poplar stand ($R^2 = 0.74$ and 0.68) and shrubland ($R^2 = 0.31$ and 0.49) sites. The comparison between GPP obtained from the eddy covariance tower (GPP_{tower}) and GPP obtained from MVPM (GPP_{MVPM}) (predicted GPP) showed good agreement for the typical steppe site of Xilinhaote ($R^2 = 0.84$ and 0.70 in 2006 and 2007, respectively) and for the Duolun steppe site ($R^2 = 0.63$) and cropland site ($R^2 = 0.63$) in 2007. The predictive power of the MVPM model decreased slightly in the desert steppe at the irrigated poplar stand ($R^2 = 0.56$ and 0.47 in 2006 and 2007 respectively) and the shrubland ($R^2 = 0.20$ and 0.41). The results of this study demonstrate the feasibility of modelling GPP from EC towers in semi-arid regions.

1. Introduction

Estimating regional carbon fluxes and stocks is an emerging research priority because of their substantial variability among regions across the globe (IPCC 2007). Two widely applied approaches to carbon flux estimation are (1) remote sensing of land-surface properties (e.g. described by Xiao et al. (2011)) and (2) applications of ecosystem models (e.g. by Jung et al. (2010)). Here, we focus on the grassland region of Inner Mongolia, China.

Grasslands, which account for 32% of global vegetation (Parton et al. 1995), are under serious pressure in Asia from the coupled effects of climate change and a growing population (Ojima et al. 1998). Semi-arid grasslands in northern China, most of which are in Inner Mongolia, make up 41% of the country's land area, and are especially prone to degradation on account of the consistent warming trends in Northeast Asia over the past 50 years (Chase et al. 2000; Lu et al. 2009) and an increase in grazing-related economic activities (Kang et al. 2007). These climatic changes (Zhai et al. 1999; Hu, Yang, and Wu 2003; Zhai and Pan 2003) have affected the productivity and stability of these semi-arid grasslands, which are under increasing pressure from an intensification of overgrazing and irrigated agriculture leading to their degradation and desertification (Zhou, Wang, and Wang 2002; Christensen et al. 2004; John et al. 2009). Such degradation has led to a dramatic modification of biophysical properties, which include albedo, leaf area index (LAI), surface roughness, soil water holding capacity, and soil moisture content, which have the potential to bring about significant changes in the regional climate (Li et al. 2000; Chen et al. 2009; Miao et al. 2009). Although grasslands play an important role in carbon sequestration, there have been very few attempts to model carbon and water fluxes in arid and semi-arid areas (Baldocchi et al. 2001).

The eddy covariance (EC) method, used for continuous, automated, on-site observations of carbon, water, and energy fluxes, has helped to obtain timely net ecosystem exchange (NEE) data that, in turn, provide gross primary production (GPP) and ecosystem respiration (R_e) estimates (Falge et al. 2002). Although the EC technique is meant to represent various types of terrestrial ecosystems, a major limiting factor is that the sampling footprint is limited to a kilometre or less (Osmond et al. 2004). In addition, these measurements are limited to homogenous, flat terrain, while logistic issues hinder the installation of sensors, especially in remote areas (Running et al. 1999). Satellite remote-sensing data provide a practical and objective method to obtain synoptic coverage of the spatio-temporal dynamics of ecosystems. In the recent past, many studies have attempted to effectively model estimates of GPP from EC towers using remote-sensing data to estimate the regional carbon budget (Aalto, Ciais, and Chevillard 2004; Turner et al. 2006; Xiao et al. 2011). Remote-sensing-based studies (terrestrial uptake and release of carbon (TURC), Moderate Resolution Imaging Spectroradiometer daily photosynthesis (MODIS-PSN), and the Global Production Efficiency Model (GLO-PEM)) have used ecosystem production efficiency to estimate GPP at regional scales (Goetz et al. 1999; Ruimy, Kergoat, and Bondeau 1999; Running et al. 2004). Although satellite remote sensing can estimate aboveground estimates of GPP or net primary production (NPP) through light-use efficiency (LUE) models that use direct measurements of vegetation indices derived from surface reflectance of the vegetation canopy, it cannot validate ecosystem respiration or NEE as respiration is obtained indirectly from process-based models that use the Q10 function, which is an indication of temperature sensitivity and soil moisture (Running et al. 1999). Production efficiency models (PEMs) usually estimate GPP as a product of photosynthetically active radiation (PAR) (the amount of incident solar radiation reaching the canopy; McCree 1972), canopy fPAR (fraction of PAR absorbed by the canopy), and LUE (ε_g). These models usually consider fPAR as a linear function of the normalized difference vegetation index (NDVI) (Tucker 1979). However, the traditional use of NDVI to model GPP is constrained by its sensitivity to soil background signature in semi-arid regions with 50% fractional cover (Huete et al. 2002). A satellite remote-sensing-based vegetation photosynthesis model (VPM) has been developed and tested for GPP modelling in different ecosystems that include evergreen conifers, temperate deciduous forest, seasonal tropical forests, and alpine meadows (Xiao et al. 2004a, 2004b, 2005; Li et al. 2007).

The VPM model is an improvement over legacy NDVI-driven PEMs in that it uses the enhanced vegetation index (EVI) as a function of fPAR. VPM also uses the land-surface water index (LSWI) along with *in situ* measurements of air temperature (T_a) and PAR from EC towers.

In addition to validating GPP estimates of the VPM model, we also tested the modelling ability of our modified VPM (MVPM), which runs solely on MODIS-derived biophysical variables that are independent of EC tower measurements. This model offers a cost-effective method of obtaining an estimate of GPP when an EC tower or climate station is not readily available at the site of interest. Since the modelling of carbon fluxes has not been extensively evaluated or applied in arid and semi-arid grassland ecosystems, we chose a network of EC tower sites across the temperate semi-arid steppe in Inner Mongolia as our field study area. The objectives of this research are to (1) evaluate the response of vegetation indices (EVI and NDVI) to the seasonal dynamics of carbon exchange in semi-arid grassland ecosystems, (2) further evaluate the ability of the VPM model for estimating the primary productivity of semi-arid grassland ecosystems, and (3) test and validate the MVPM model, independently of the EC tower measurements. This study provides validation of two broadly used GPP models in semi-arid regions in both natural and agricultural ecosystems.

2. Methods

2.1. Study sites

This study was conducted in Inner Mongolia, China, characterized by the continental, semi-arid monsoon climate of eastern Eurasia, with a growing season that starts in April and ends in early October. Our study sites consist of a network of five EC towers in (1) a typical steppe (D01) and cropland (D02) tower pair in Duolun, (2) a heavily grazed steppe at Xilinhaote (X03), and (3) a pair of EC towers in the desert steppe at Kubuqi with one tower in an irrigated poplar stand (K04) and the other in the surrounding shrubland (K05) (Figure 1, Table 1).

The Duolun sites are located within the Duolun Restoration Ecology Research Station, of which ~50 ha has been fenced off since 2001 to exclude grazing. The Duolun EC towers are located in an agro-pastoral typical steppe with long-term climatic data indicating an annual mean temperature of 5.2°C and with mean monthly temperatures ranging from –15.9°C in January to 19.9°C in the peak growing season. The mean annual precipitation is 399 mm with maximum precipitation in July or August. The typical steppe is dominated by *Stipa krylovii*, *Artemisia frigida*, *Cleistogenes squarrosa*, and *Leymus chinensis* and is characterized by an annual precipitation of 350 mm or less (Kang et al. 2007). The cropland site was previously a typical steppe until it was converted to agricultural fields in which *Triticum aestivum* L., *Avena nuda* L., and *Fagopyrum esculentum* Moench are planted in mid-May and harvested in mid-September. The EC tower in Xilinhaote is also located in the typical steppe where livestock grazing is the primary land use with heavy degradation of the steppes due to overgrazing. The mean annual temperature here is 7.2°C, with January and July being the coldest and hottest months (–22.3 and 18.8°C, respectively). The EC towers are within a fenced area of the Inner Mongolia Grassland Ecosystem Research Station (IMGERS, Chinese Academy of Sciences) and have an annual precipitation of 400 mm.

The two Kubuqi towers were erected in a 3 year-old poplar plantation and the surrounding shrubland. This region is around 400 km long and 50 km wide, between the southern bank of the Yellow River and the northern portion of the Ordos plateau (~1000 m a.s.l.). The desert steppe is characterized by the continental type of climate with an annual
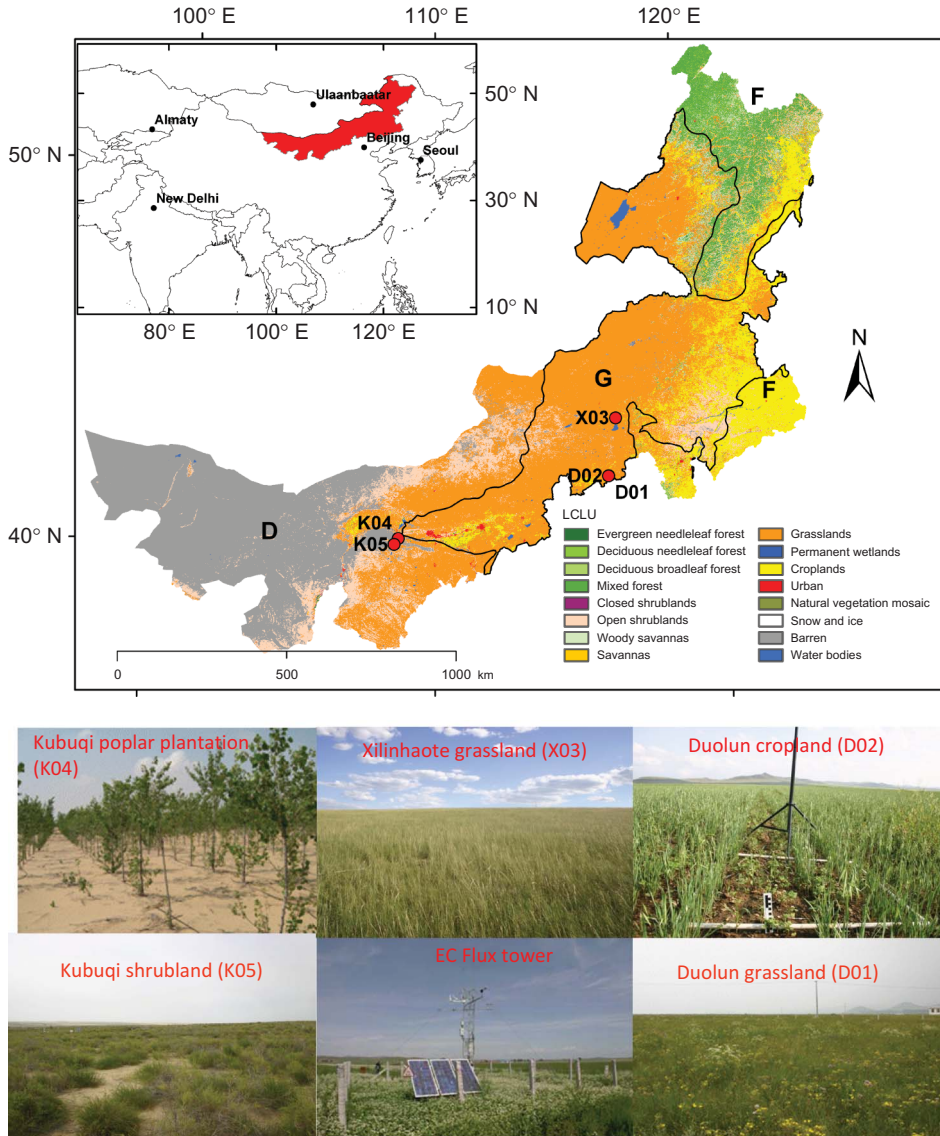
Figure 1. Land-cover land-use (LCLU) map of Inner Mongolia, People's Republic of China, over-laid with terrestrial ecoregion biome boundaries, desert (D), grassland (G), forest (F), and flux tower sites in Duolun (D01 and D02), Xilinhaote (X03), and Kubuqi (K04 and K05); units are in kilometres.

precipitation of 150–200 mm. Mean monthly temperatures range between –11°C and 24°C in January and July, respectively, based on data from nearby meteorological stations from 1957 to 2000 (Nos. 53336, 53446, 53513, 53529, 53543; China Meteorological Data Sharing Service System, http://cdc.cma.gov.cn, China Meteorological Administration). As a dune stabilization measure, ∼200 km^2 were planted with poplar in 1998 (Wilske et al. 2009). These young poplars have a mean height of 1.5–2.0 m with an intercrop of *Glycyrrhiza uralensis* Fisch. The plantation near the EC tower covered an area of 3.73 km^2. Tree height and LAI varied greatly as some trees had grown to a height of 4 m, whereas

Table 1. Site location and characteristics of five flux towers in Inner Mongolia, China, in 2006–2007.

Site	Vegetation	Location			Annual rainfall (mm)		Mean annual temperature (°C)	
		Latitude (°N)	Longitude (°E)	Altitude (m)	2006	2007	2006	2007
D01	Duolun steppe	42.046667	116.283610	1350	423.0	199.0	3.8	3.5
D02	Duolun cropland	42.045556	116.279722	1350	414.0	190.0	5.2	3.4
X03	Xilinhaote steppe	43.554444	116.671389	1250	190.0	170.4	7.2	4.2
K04	Kubuqi poplar	40.563333	108.745000	1020	152.0	180.4	11.0	8.4
K05	Kubuqi shrubland	40.451667	108.625000	1160	226.0	197.0	10.6	7.7

others exhibited stunted growth. The water table varied between 1 and 4 m deep, depending on the height of the sand dunes. The poplar plantation is provided with drip irrigation during droughts, with irrigation periods lasting for about 11 hours. Water equal to precipitation of 1.46 mm was supplied during each period – nine times from April through September, 2005. Drip irrigation in 2006 was provided twice in April, once in May, and once in June, with similar frequency in 2007.

The second EC tower at Kubuqi is located 20 km south of the poplar plantation tower in a native shrubland. The shrubland matrix is dominated by shrub species *Artemisia ordosica* Krasch and *Hedysarum mongolicum* Turcz. The *Artemisia ordosica* found here is a deciduous shrub with a height of 0.6–1.0 m (Wilske et al. 2009) with fractional cover of 15–23%. It is important to note that the soil moisture at the Kubuqi shrubland tower site was twice as high as the irrigated poplar site (Wilske et al. 2009).

The EC flux towers at the aforementioned sites measured fluxes of carbon dioxide (CO_2), latent heat, and sensible heat at 4 m height (Chen et al. 2009). The flux data were processed with EC_Processor (Noormets, Chen, and Crow 2007) using a planar fit coordinate rotation (Wilczak, Oncley, and Stage 2001) that included temperature and pressure corrections for sonic temperature (Schotanus, Nieuwstadt, and De Bruin 1983), air density (Webb, Pearman, and Leuning 1980), and additional heat flux (Burba et al. 2008) corrections for turbulent fluxes. Daily totals of NEE, R_e, and gross ecosystem productivity (GEP) were calculated from quality-checked (Foken and Wichura 1996) and gap-filled data using non-linear functional regression models (Moffat et al. 2007). Different parameterizations of the light- and temperature-response functions were used for the active and dormant seasons, which were delineated according to soil temperature at 5 cm with a threshold of 3°C. Additional meteorological data measured at each site included net radiation, PAR, temperature, and relative humidity at 30 min intervals. The flux tower data were collected half-hourly, with 26–33% data coverage in 2006 and 34–26% data coverage in 2007, which were not gap-filled, with 80% of all gaps occurring in night-time. The gap-filled data compared favourably with other studies that used the same flux towers (Chen et al. 2009; Miao et al. 2009). Falge et al. (2001) reported that random error for daytime NEE estimates was 3.5–20% and the time-integrated error for annual estimates was 8.3–11%. Meteorological data collected at the towers were checked against independent measurements by nearby meteorological stations operated by the China Meteorological Administration. These include station 54208, 22 km northeast of D01 and D02; station 54102, 60 km northwest of X03; station 53336, 118 km north of K04; and station 53529, 151 km southwest of K05.

2.2. Satellite data

We analysed a time series of imagery from the morning overpass of the MODIS sensor aboard the Terra satellite (crossing the equator at 10:30 AM). We acquired 8 day composites of MODIS-derived surface reflectance (MOD09A1 v005) from the NASA Warehouse Inventory Search Tool data gateway (https://wist.echo.nasa.gov/api/). Of the seven spectral bands in MOD09A1 used to study vegetation and land-surface properties, we used the blue (459–479 nm), green (545–565 nm), red (620–670 nm), near-infrared (NIR) (841–875 nm), and shortwave infrared (SWIR) (1628–1652 nm) bands to derive the spectral indices (EVI, NDVI, and LSWI) for the VPM and MVPM models. In addition, we acquired 8 day composites of MODIS-derived biophysical variables such as GPP (MOD17A2 v005), fraction of photosynthetically active radiation (fPAR) (MOD15A2 v005), and land-surface temperature (LST) (MOD11A2 v005). The improved GPP data from the University of Montana's Numerical Terradynamic Simulation Group (NTSG) were used in addition to the latest Collection 5 version of MODIS fPAR (MOD15A2 v005), instead of the older, Collection 4 version of MOD17A2, which is sensitive to cloud and aerosol contamination in the Collection 4 fPAR/LAI product (Zhao et al. 2005). The MODIS GPP (GPP$_{MODIS}$) is calculated based on an LUE model (Running et al. 2004):

$$GPP_{MODIS} = \varepsilon_{max} m(T_{min}) \times m(VPD) \times (f PAR) \times (SW) \times 0.45, \qquad (1)$$

where ε_{max} is the maximum LUE and $m(T_{min})$ and $m(VPD)$ are scalars that lower ε_{max} under stressful conditions of low temperature and high vapour pressure deficit (VPD), respectively. SW is the shortwave radiation component, and fPAR is the fraction of PAR. While ε_{max} is derived from a lookup table, T_{min}, VPD, and SW are obtained from coarse resolution NASA Data Assimilation Office (DAO) datasets.

2.3. VPM model

2.3.1. Vegetation photosynthesis model

The fraction of light absorbed by the canopy (fPAR$_{canopy}$) is partitioned into the fraction of light absorption by chlorophyll (fPAR$_{chl}$) and non photosynthetic vegetation (NPV) (fPAR$_{NPV}$). Based on this, Xiao et al. (2004a, 2004b) developed the VPM model, which differs slightly from the MODIS GPP equation. Instead of the BPLUT lookup table, which in turn was derived from the BIOME-BGC model (Turner et al. 2005), the LUE, ε_g, is obtained from remote-sensing inputs and meteorological inputs as follows:

$$GPP = \varepsilon_g \times (f PAR_{chl}) \times (PAR), \qquad (2)$$

$$\varepsilon_g = \varepsilon_0 T_{scalar} W_{scalar} P_{scalar}, \qquad (3)$$

where PAR is the photosynthetically active radiation (μmol m^{-2} s^{-1}), fPAR$_{chl}$ is the fraction of PAR absorbed by chlorophyll, and ε_g is the LUE (μmol CO$_2$ PAR^{-1}, i.e. the amount of carbon dioxide that vegetation can produce per unit energy). The parameter ε_0 is the maximum LUE (μmol PAR) and T_{scalar}, W_{scalar}, and P_{scalar} are the regulation scalars for the effects of temperature, water, and leaf phenology on the LUE of vegetation.

The input data for simulation of the VPM model include remote-sensing data (e.g. from MODIS or the Système Pour l'Observation de la Terre (SPOT) vegetation sensor), air

temperature, PAR, and vegetation type (deciduous and evergreen, C_3 and C_4 plants). It was proposed that fPAR$_{chl}$ can be estimated as a linear function of the EVI, which uses surface-reflectance values (where ρ_{nir}, ρ_{red}, and ρ_{blue} are the reflectances in the near-infrared, red, and blue bands, respectively). The coefficient a is set to 1.0 (Xiao et al. 2004a, 2004b).

$$f\mathrm{PAR}_{chl} = a \times (\mathrm{EVI}), \tag{4}$$

$$\mathrm{EVI} = \frac{\rho_{nir} - \rho_{red}}{\rho_{nir} + 6\rho_{blue} - 7.5\rho_{red} + 1}. \tag{5}$$

Because the short-infrared spectral band is sensitive to vegetation water content and soil moisture, a combination of NIR and SWIR bands have been used to derive water-sensitive vegetation indices, including the LSWI. LSWI values vary from –1 to +1.

$$\mathrm{LSWI} = \frac{\rho_{nir} - \rho_{swir}}{\rho_{nir} + \rho_{swir}}, \tag{6}$$

where ρ_{swir} is the reflectance in the short wave-infrared. As leaf liquid water content increases or soil moisture increases, SWIR absorption increases and SWIR reflectance decreases, resulting in an increase in LSWI. Recent work in evergreen needleleaf as well as temperate broadleaf forests has shown that LSWI is sensitive to changes in leaf water content (equivalent water thickness) over time (Xiao et al. 2004a, 2004b).

W_{scalar}, T_{scalar}, and P_{scalar} are down-regulation scalars that describe the effects of water, temperature, and leaf phenology, respectively, on the LUE of vegetation. The seasonal dynamics of W_{scalar} are obtained as:

$$W_{scalar} = \frac{1 + (\mathrm{LSWI})}{1 + (\mathrm{LSWI})_{max}}, \tag{7}$$

where LSWI$_{max}$ is maximum LSWI of the growing season. T_{scalar} is a measure of the sensitivity of photosynthesis to temperature, calculated at each time step using the equation developed for the Terrestrial Ecosystem Model (Raich et al. 1991):

$$T_{scalar} = \frac{(T - T_{min})(T - T_{max})}{[(T - T_{min})(T - T_{max})] - (T - T_{opt})^2}, \tag{8}$$

where T_{min}, T_{max}, and T_{opt} are minimum, maximum, and optimal temperatures (0°C) for photosynthesis, respectively. If air temperature falls below T_{min}, T_{scalar} is set to zero. P_{scalar} accounts for the effects of leaf phenology on photosynthesis at the canopy level.

$$P_{scalar} = \frac{1 + (\mathrm{LSWI})}{2}. \tag{9}$$

The calculation of P_{scalar} is dependent upon the longevity of the leaves (deciduous when compared to evergreen). Since a grassland canopy has new leaves through the growing season, the value of P_{scalar} is set to 1.

2.3.2. *VPM model parameterization*

The VPM model has four important parameters: (1) maximum LUE; (2) the effect of temperature on vegetation photosynthesis (T_{scalar}) as governed by minimum, maximum, and optimal temperature measurements; (3) the effect of water on photosynthesis (W_{scalar}), which is represented by the maximum LSWI of the growing season; and (4) the effect of phenology (P_{scalar}) on photosynthesis.

The LUE (ε_g) varies by ecosystem type and can be obtained through meta-analysis from the published literature or can be estimated through a nonlinear regression of site-specific NEE with PAR data within the growing season (Xiao et al. 2004a, 2004b; Li et al. 2007). Maximum LUE (ε_0) varies with vegetation type and can be obtained from the NEE of CO_2 flux and incident PAR. We derived maximum ε_0 for the different ecosystem types through nonlinear models with the best fit based on the Michaelis–Menten function between NEE and PAR during the peak period of the active growing season (Table 2).

T_{scalar} was obtained by analysing the relationship between temperature and daily GPP. Temperature is an important control on GPP, as a sufficient but not extreme temperature is required for photosynthesis. Photosynthesis increases until an optimal temperature range, beyond which it begins to decrease. This optimal range is quite large, and we established the limiting temperatures based on the relationship between photosynthesis and air temperature measured at the tower sites. In 2006, we estimated a minimum temperature of 1°C and an optimal temperature of 17°C, with a maximum temperature of 29.7°C at D01, 30.7°C at D02, 31.7°C at X03, 35.8°C at K04, and 37.7°C at K05. In 2007, we estimated a minimum of 1°C temperature, whereas optimal temperatures ranged between 18.5°C at D01 and 23.5°C at K05. The maximum temperatures in 2007 were 23.9°C at D01, 28.1°C at D02, 29.4°C at X03, 27°C at K04, and 27.4°C at K05 (Table 2).

W_{scalar} is obtained through the selection of the site-specific maximum LSWI value (LSIW$_{max}$) in the active growing season. We did not use the annual LSWI$_{max}$ as winter LSWI values are extremely high, owing to snow cover and are therefore excluded. In 2006, LSWI$_{max}$ varied among sites with peak values of 0.2 in the Duolun steppe, 0.2 in the Duolun cropland, and –0.01 in the Xilinhaote grassland on 28 July 2006. In the desert steppe, maximum LSWI values were –0.05 in K04 and 0.05 in K05 on 22 September and 29 August, respectively. LSWI$_{max}$ in 2007 varied between sites with values of 0.04 in D01, 0.08 in D02, and –0.003 on 28 July, 21 August, and 5 August, respectively. In the desert steppe, LSWI$_{max}$ of 0.008 at K04 and –0.035 at K05 were reached on 20 July (Table 2).

P_{scalar} accounts for the effects of phenology on photosynthesis at the canopy level. The calculation of P_{scalar} is dependent upon the longevity of the leaves (deciduous vs.

Table 2. Site-level parameters used in VPM model that include maximum air temperature ($T_{a\,max}$), optimal air temperature ($T_{a\,optimal}$), maximum LUE, LSWI$_{max}$, and associated standard error estimates.

Site	$T_{a\,max}$ 2006	$T_{a\,max}$ 2007	$T_{a\,optimal}$ 2006	$T_{a\,optimal}$ 2007	LUE (μmol CO_2 m^{-2} s^{-1}) 2006	SE	2007	SE	LSWI$_{max}$ 2006	LSWI$_{max}$ 2007
D01	29.6	17.1	17.0	18.5	0.0327	0.0040	0.0233	0.0144	0.22	0.040
D02	30.67	28.1	17.0	23.5	0.0318	0.0047	0.0314	0.0146	0.22	0.080
X03	31.72	25.5	17.0	23.0	0.0416	0.0063	0.0473	0.0100	−0.01	−0.003
K04	35.85	23.1	17.0	22.0	0.0723	0.0246	0.0330	0.0090	−0.05	0.008
K05	37.71	29.4	17.0	23.5	0.1166	0.0466	0.0330	0.0431	0.05	−0.035

evergreen). Since a grassland canopy has new leaves throughout the growing season, the P_{scalar} is set to 1 for D01, D02, and X03. However, for the irrigated poplar stand and shrubland sites, K04 and K05, we computed P_{scalar} as a linear function of LSWI from budburst to leaf expansion, after which it is set to 1.

2.4. *Modified vegetation photosynthesis model*

The model is based on the LUE models, where GPP is linearly related to the product of PAR and the efficiency with which the absorbed light is used to fix carbon (Running et al. 2004). Early LUE models (Monteith 1972) assumed that LUE was constant; however, recent studies have shown that LUE varies considerably across ecosystem types and environmental stochasticity such as drought and diffuse albedo (Ruimy, Saugier, and Dedieu 1994). GPP models generally estimate LUE through the use of lookup tables of LUE for a given biome type (Running et al. 2004). This can lead to errors owing to the coarse resolution ($1.00° \times 1.25°$ pixels) in the meteorological data from the DAO and the spatial mismatch with the higher resolution (1 km) of the MODIS GPP data (Zhao et al. 2005). It would be much simpler, from a processing point of view, to create a GPP model based entirely on remotely sensed data of similar resolution and of the same spatial scale.

Previous studies have suggested that independent measures of LUE were unnecessary as they found good correlations between satellite-derived spectral indices with carbon fluxes as well as with LUE (Sims et al. 2006a). Although most of the early studies showing good correlations between spectral indices and primary productivity were integrated over growing season composites (Goward, Tucker, and Dye 1985), it remains unclear to what extent short-term variability in carbon fluxes can be estimated through spectral indices (Sims et al. 2006b). Although some GPP modelling studies in semi-arid areas using correlations between NDVI and carbon fluxes have been carried out (Wylie et al. 2003), they have not been measured extensively across different ecosystem types (Sims et al. 2006b).

An important limitation of the VPM model is that it is not entirely independent of ground-based sensor measurements such as PAR and temperature. We studied the feasibility of replacing these variables with MODIS-derived GPP, fPAR, and LST products. In the following equation, we modify GPP_{MODIS} by multiplying it with a suite of MODIS-derived variables, EVI, LSWI, and LST, which are surrogates of productivity, water content, and temperature, respectively, and then dividing the product with fPAR $_{MODIS}$. We based this on Monteith's (1972) widely accepted LUE model, where LUE = $(GPP)/(f$PAR$) \times$ PAR.

We include LSWI and LST as down-regulation scalars of GPP as our study area is predominantly a water-limited semi-arid ecosystem. Although the inclusion of LSWI as a down-regulation scalar draws from the VPM model, we included the LST based on the temperature and greenness model (Sims et al. 2008), which found a strong correlation between both VPD and PAR with surface temperature and is said to have substantially improved predictions of GPP when compared to the standard MODIS GPP product.

$$GPP_{MVPM} = [\ln(GPP_{MODIS}) \times (EVI) \times (LSWI) \times (LST)]/(f PAR_{MODIS}). \qquad (10)$$

We log-transferred GPP_{MODIS} in our regression analysis because tower GPP may reflect only a fraction, and possibly a nonlinear relationship with GPP_{MODIS}, which is an aggregate measure over the 8 day period.

2.5.   Uncertainty analysis

We used three metrics to evaluate the performance of the VPM and MVPM models as well as GPP_{MODIS}. They include: (1) the coefficient of determination (R^2), which represents the amount of observational variance explained by the regression model; (2) predictive error (PE), which is a measure of the difference between observed and predictive values; and (3) root mean square error (RMSE), which is the standard error of the estimate in regression analysis and a measure of precision. We compared GPP_{MODIS}, GPP_{VPM}, and GPP_{MVPM} with GPP obtained from eddy covariance tower (GPP_{tower}) seasonally integrated sums during the active growing season (May–October) and at annual intervals. We validated the accuracy of the two satellite-derived GPP models and MODIS products with emphases on maximum values and annual and interannual variations. In addition, we evaluated the different sensitivities of EVI and NDVI to GPP_{tower} using the procedure outlined in Gitelson (2004). We used Equation (11):

$$S = [\mathrm{d}(EVI)/\mathrm{d}(NDVI)] \times [\Delta(EVI)/\Delta(NDVI)]^-, \tag{11}$$

where $\mathrm{d}(EVI)$ and $\mathrm{d}(NDVI)$ are the first derivatives of the indices with respect to GPP_{tower} and $\Delta EVI = (EVI)_{max} - (EVI)_{min}$ and $\Delta(NDVI) = (NDVI)_{max} - (NDVI)_{min}$ are the differences between the minimum and maximum vegetation index values in the growing season. Values of $S < 1$ could be interpreted as NDVI being more sensitive than EVI, and values of $S > 1$ indicate that EVI was more sensitive to GPP_{tower}. The sensitivities of both EVI and NDVI were considered to be equal when $S = 1$.

It is a widely recognized fact that parameter estimation in biophysical models is susceptible to various sources of uncertainty (Aber 1997), and in the absence of field measurements for all of the parameters, we relied on the published literature to provide error estimates for some of the MODIS standard products used in the VPM and MVPM models. The MVPM model is based on vegetation and water content indices, EVI and LSWI, derived from Collection 5 surface reflectance (MOD09A1V005), which is atmospherically corrected to reduce attenuation due to aerosol scattering and gaseous absorption (Vermote, El Saleous, and Justice 2002). A maximum value compositing (MVC) technique is used to screen for poor quality pixels resulting from extreme off-nadir look angles and cloud cover (Vermote, El Saleous, and Justice 2002). The quality of MOD09A1 Collection 5 has been significantly improved when compared to Collection 4 and was validated at 150 Aerosol Robotic Network (AERONET) sites (Vermote and Kotchenova 2008). Error estimates for MOD09A1 from Terra were reported to be $\pm 0.005 + 5\%$ and the percentage of good observations of MODIS bands 1, 2, 3, 4, 5, 6, and 7 were 88.66%, 94.34%, 50.52%, 79.34%, 96.50%, 97.87%, and 98.62%, respectively (Vermote and Kotchenova 2008). The study also obtained error estimates for vegetation indices derived from the MOD09 product with up to 97.11% of NDVI values and 93.64% of EVI values falling within the one-sigma error bar: $\pm 0.02 + 0.02(VI)$, where 'VI' is the vegetation index (Vermote and Kotchenova 2008).

The LST (MOD11A2V005), defined as the radiance emitted by the land surface as measured by MODIS, has been validated extensively over different land-cover types, which include lakes, grassland/rice fields in California, and silt playas in New Mexico, with errors of 0.2 K, 0.5 K, and 0.9 K, respectively (Wan, Zhang, and Li 2002). It is important to note that LST or T_{skin} differs from air temperature (T_{air}), although both are complementary in climate change studies (Jin and Dickinson 2010). This difference was highlighted by Wan et al. (2004) and Wan (2008), where LSTs differed from *in situ* measurements at a silt valley playa at Railroad Valley in Nevada, USA, as surface emissivities in semi-arid and

arid regions can often be overestimated, especially in bare soil sites. A major improvement in Collection 5 MODIS LST was that cloud-contaminated pixels were kept to a minimum with accuracy compared to *in situ* measurements being within 1 K with an RMSE of 0.7 (Wan 2008).

We used MODIS *f*PAR Collection 5, which is a significant (MOD15A2V005) improvement over the Collection 4 product version that utilized a turbid medium radiative transfer model to estimate LAI, *f*PAR, and Collection 3 land-cover product (Shabanov et al. 2007). Turner et al. (2006) stated that rigorous validation of MODIS *f*PAR was done at only a few sites (e.g. northern Senegal, Australia, etc.), mostly in ecosystems with low *f*PAR (Fensholt, Sandholt, and Rasmussen 2004; Kanniah et al. 2009). Some of the drawbacks of these validations were that LAI measurements were converted to *f*PAR based on Beer's law, without taking into account the canopy structure or solar geometry (Turner et al. 2006). Although Collection 4 MODIS *f*PAR successfully tracked seasonal variations (Fensholt, Sandholt, and Rasmussen 2004) and was sensitive to changes in vegetation following disturbance like fire (Kanniah et al. 2009), it overestimated *in situ* measurements with an overall offset of 0.22, with the highest values estimated in a range of 0.06–0.15, i.e. approximately 10–20% in Sahelian grasslands (Fensholt, Sandholt, and Rasmussen 2004). The Collection 5 MODIS *f*PAR product used a new stochastic radiative transfer (RT) model, which allowed for a better characterization of canopy structure and spatial heterogeneity and used a new Collection 4 land-cover product (Shabanov et al. 2007). A new Biome Parameter Lookup Table in Collection 5 ensured the consistency between measured and simulated MODIS surface reflectance, with uncertainty levels for spectral bands, resulting in minimal overestimation of LAI and *f*PAR over sparse vegetation (Shabanov et al. 2007).

3. Results

3.1. Seasonal dynamics of vegetation indices and tower GPP

The seasonal dynamics of GPP are driven by temperature and PAR in these temperate steppes with GPP_{tower} values near zero in the winter season – day-of-year (DOY) ranging from 1 to 113 and from 297 to 365 – owing to the absence of photosynthetic activity (Figure 2). The GPP_{tower} time series for 2006–2007 had a seasonal cycle with distinct differences in phase and amplitude (Figure 3). There were temporary decreasing trends in the GPP_{tower} time series (Figure 3), owing to low temperature and low values of PAR during rainy days (Figure 2).

The growing season began on 23 April (DOY 113) with an increase in PAR and air temperature leading to growth in vegetation and a subsequent increase in the ecosystem's photosynthetic capacity (Figure 2). EVI and NDVI follow the increase in GPP_{tower} closely until the growing season peak is reached in late July (DOY 185–217), after which the GPP_{tower} declines. There is a subsequent decrease in EVI and NDVI, as vegetation senesces with a decrease in temperature and PAR availability.

The relative sensitivity of the EVI and NDVI dynamic ranges in response to changes in GPP_{tower} showed that all five sites had *S* values greater than 1 in both the 2006 and 2007 growing seasons, indicating that the EVI was slightly more sensitive to changes in GPP_{tower} than NDVI was, with the exception of X03 in 2007, where *S* was equal to 0.95 (Table 3). It is important to note that K04 and K05 in the desert steppe had higher *S* values than the other sites (i.e. EVI was more sensitive to GPP_{tower} than NDVI was at the xeric sites).
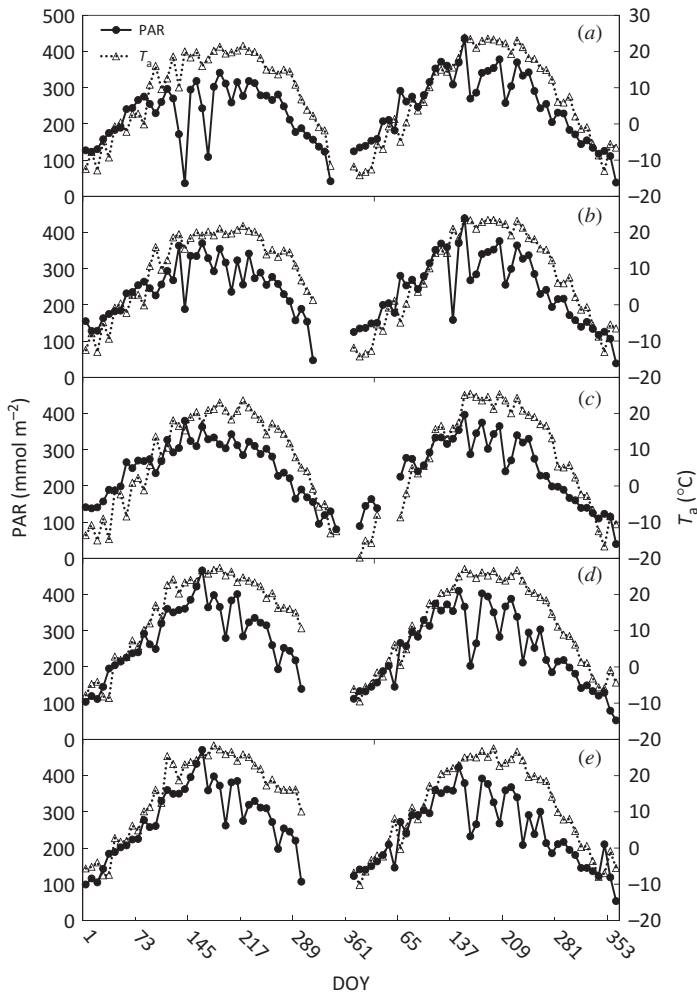
Figure 2. Seasonal changes for growing seasons of 2006 and 2007 in PAR and air temperature (T_a) in (*a*) Duolun steppe, (*b*) Duolun cropland, (*c*) Xilinhaote steppe, (*d*) Kubuqi poplar plantation, and (*e*) Kubuqi shrubland.

The photosynthetic capacity of the different land-cover/land-use (LCLU) types varied between the two years. In 2006, D01 and D02 had peak values of 3.07 g C m^{-2}day^{-1} (grams of carbon per square metre per day) and 8.71 g C m^{-2}day^{-1} (Figures 3(*a*) and (*b*)), respectively, while their total GPP$_{tower}$ was 40.00 and 77.00 g C m^{-2} year^{-1}, respectively. The X03 site had a peak value of 3.00 g C m^{-2}day^{-1} (in July (Figure 3(*c*)) and a total GPP$_{tower}$ value of 49.62 g C m^{-2} year^{-1}. The K04 and K05 sites had peak GPP$_{tower}$ values of 2.97 and 1.41 g C m^{-2}day^{-1} (Figures 3(*d*) and (*e*)), while their total GPP$_{tower}$ values were 45.44 and 30.24 g C m^{-2} year^{-1} in the annual growing season, respectively (Table 4).

In contrast, GPP$_{tower}$ in 2007 was slightly less compared to 2006. This difference is especially true for D01 and D02, with peak values of 1.30 and 1.90 g C m^{-2}day^{-1}, respectively (Figures 3(*a*) and (*b*)), with annually integrated GPP$_{tower}$ values of 24.00 and 27.65 g C m^{-2} year^{-1}, respectively (Table 4). The 2007 peak season in X03 was reached a
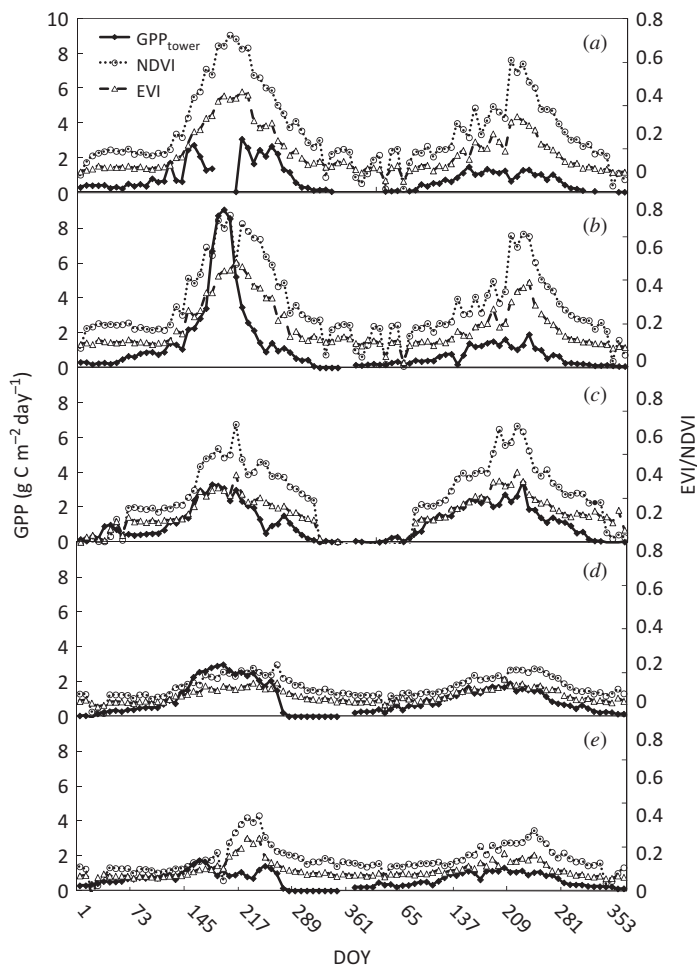
Figure 3. Seasonal changes in observed GPP$_{tower}$ and MODIS-derived NDVI and EVI in (*a*) Duolun steppe, (*b*) Duolun cropland, (*c*) Xilinhaote steppe, (*d*) Kubuqi poplar plantation, and (*e*) Kubuqi shrubland.

Table 3. The relative sensitivity of EVI and NDVI to changes in GPP$_{tower}$, expressed by the function, $S = [d(EVI)/d(NDVI)] \times [\Delta(EVI)/\Delta(NDVI)]^{-1}$.

Site	2006	2007
D01	1.151	1.136
D02	1.018	1.027
X03	1.065	0.952
K04	1.370	1.054
K05	1.358	1.235

Notes: Values of $S < 1$ indicate that NDVI is more sensitive than EVI, whereas values of $S > 1$ indicate that that EVI was more sensitive to changes in GPP$_{tower}$. The sensitivities of both EVI and NDVI were considered to be equal when $S = 1$.

Table 4. Observed GPP$_{tower}$ when compared with predicted GPP$_{VPM}$ and GPP$_{MVPM}$ (g C m^{-2} year^{-1}) in five semi-arid LCLU types.

| | Flux tower | | | | VPM | | | | MVPM | | | | MODIS GPP | | | |
| | GPP$_{obs\,(1–12)}$ | | GPP$_{obs\,(5–10)}$ | | GPP$_{pre\,(1–12)}$ | | GPP$_{pre\,(5–10)}$ | | GPP$_{pre\,(1–12)}$ | | GPP$_{pre\,(5–10)}$ | | GPP$_{pre\,(1–12)}$ | | GPP$_{pre\,(5–10)}$ | |
Site	2006	2007	2006	2007	2006	2007	2006	2007	2006	2007	2006	2007	2006	2007	2006	2007
D01	40.00	24.00	33.20	21.41	69.42	29.43	68.00	28.40	78.90	62.41	79.08	61.58	29.32	23.02	28.26	21.73
D02	77.00	27.65	69.02	22.59	72.96	49.00	71.64	48.02	74.18	60.29	75.57	59.26	29.32	25.42	28.43	23.96
X03	49.62	50.14	42.18	43.67	59.36	70.20	57.72	68.86	49.50	54.51	49.64	53.33	23.07	25.61	22.31	24.32
K04	45.44	39.12	40.61	30.30	74.13	28.51	69.84	26.96	42.64	34.32	39.52	31.66	15.23	10.65	13.27	9.05
K05	30.24	25.40	21.43	21.50	86.28	19.31	81.76	18.13	53.20	35.95	49.21	34.62	11.72	9.38	10.48	7.93

Notes: GPP$_{obs\,(1–12)}$ and GPP$_{pre(1–12)}$ are the observed and predicted annual integrated GPP. GPP$_{obs\,(5–10)}$ and GPP$_{pre\,(5–10)}$ are the observed and predicted integrated GPP within the active growing season.

month later in August with a growing season peak value of 3.43 g C m^{-2}day^{-1} (Figure 3(c)) and an annual value of 50.14 g C m^{-2} year^{-1} (Table 4). The lagged 2007 peak season seems evident in the K04 and K05 sites with peak values, in August, of 1.80 and 1.15 g C m^{-2}day^{-1} (Figures 3(d) and (e)) and an annual GPP$_{tower}$ values of 39.12 and 25.40 g C m^{-2} year^{-1}, respectively (Table 4). Integrated GPP$_{tower}$ values in the 2007 active growing season for the months of May–October (Table 4) were significantly lower in D01, D02, and K04 when compared to 2006. However, there were no significant differences in GPP$_{tower}$ values for X03 or K05 in 2006 or 2007.

The intra-annual seasonal dynamics of vegetation indices (i.e. EVI and NDVI derived from the MODIS 8 day reflectance product) follow seasonal changes in vegetation but differ in amplitude among the different LCLU types (Figure 3). The maximum NDVI values in D01, D02, and X03 are in the range of 0.7–0.8, while the EVI values range between 0.5 and 0.6. Although the EVI and NDVI closely follow the 2006 and 2007 seasonal changes in GPP$_{tower}$ at D01, D02, X03, and K04 with the peak season in late July, the vegetation indices in the desert steppe KO5 site lag behind GPP$_{tower}$ due to a delayed peak season in response to rainfall in late August. The lag effect is especially obvious in 2007 for all five sites with the peak season being reached at the end of August.

3.2. MODIS GPP validated by tower GPP

Linear regression analysis of GPP$_{MODIS}$ with GPP$_{tower}$ estimates showed reasonable agreement and were statistically significant ($p < 0.01$) (Table 5). Although there was a strong correlation between GPP$_{MODIS}$ and GPP$_{tower}$ at the X03 typical steppe site in both 2006 and 2007, modelling efficiency decreased in the K04 and K05 towers, explaining only 40% of the variation at the desert steppe (Table 5). However, GPP$_{MODIS}$ had an R^2 of 0.49 at the K05 shrubland site in 2007, thus explaining 10% more of the variation than the other desert steppe towers (Table 5). In the D01 mesic steppe site, GPP$_{MODIS}$ explained 44% of the variation in GPP$_{tower}$ in 2006 and 61% in 2007. However, the regression model explained 55% and 67% of GPP$_{tower}$ variation in 2006 and 2007, respectively (Table 5).

GPP$_{MODIS}$ consistently underpredicted GPP$_{tower}$ at all five sites (Tables 4 and 5, Figures 4–7), with the only exceptions being the D01 typical steppe and D02 cropland in 2007 where the margin of error was minimal with PEs of –0.97 and –2.22 g C m^{-2} year^{-1},

Table 5. Comparison of model coefficient of determination (R^2), RMSE from linear regression, and PE of observed GPP$_{tower}$ with predicted GPP$_{VPM}$ and GPP$_{MODIS}$ for five semi-arid LCLU types ($p < 0.01$).

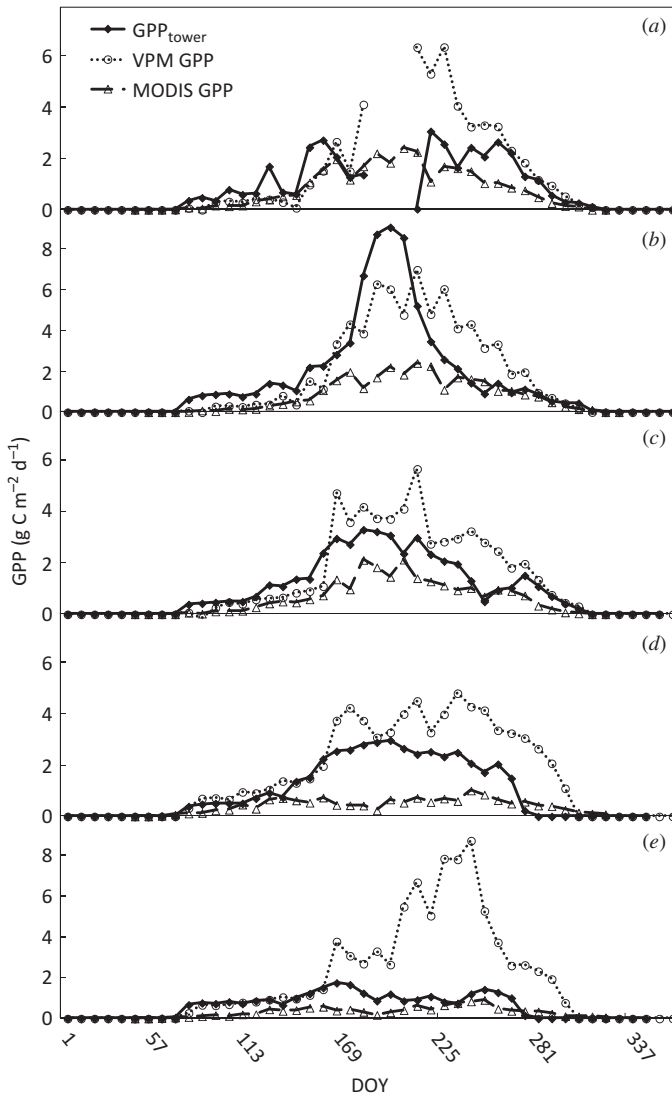| | MODIS GPP | | | | | | VPM GPP | | | | | |
| | 2006 | | | 2007 | | | 2006 | | | 2007 | | |
Site	R^2	PE	RMSE	R^2	PE	RMSE	R^2	PE	RMSE	R^2	PE	RMSE
D01	0.44	−10.67	0.51	0.61	−0.97	0.39	0.44	29.42	1.35	0.43	5.43	0.70
D02	0.55	−47.67	0.52	0.67	−2.22	0.40	0.67	−4.04	1.22	0.71	21.35	0.87
X03	0.82	−26.54	0.27	0.79	−24.52	0.30	0.80	9.74	0.72	0.73	20.06	1.10
K04	0.40	−30.20	0.20	0.44	−25.75	0.17	0.74	28.69	0.85	0.68	−10.61	0.42
K05	0.41	−18.51	0.20	0.49	−16.01	0.12	0.31	56.04	2.02	0.63	−6.09	0.20

Figure 4. A comparison of the seasonal changes in observed GPP$_{tower}$ with predicted GPP$_{VPM}$ and GPP$_{MODIS}$ at five flux sites in 2006: (*a*) Duolun steppe, (*b*) Duolun cropland, (*c*) Xilinhaote steppe, (*d*) Kubuqi poplar plantation, and (*e*) Kubuqi shrubland. The Duolun steppe tower has missing data in June and July.

respectively (Tables 4 and 5, Figure 6(*a*)). However in the previous year, GPP$_{MODIS}$ underestimated GPP$_{tower}$ with a PE bias as high as –47.67 at D02 and was not able to capture the rapid peak in GPP dynamics exhibited by the cropland site (Tables 4 and 5, Figure 4(*b*)). GPP$_{MODIS}$ underestimated GPP$_{tower}$ at the X03 typical steppe site where the predictive bias was as high as –26.54 and –24.52 g C m^{-2} year^{-1} in 2006 and 2007, respectively. In the desert steppe, the K04 irrigated poplar stand showed greater PE bias, –30.20 and –25.75 g C m^{-2} year^{-1}, in 2006 and 2007, respectively (Tables 4 and 5), when compared to the K05 shrubland site (PE of –18.51 and –16.01 g C m^{-2} year^{-1}) (Figure 6(*e*)).
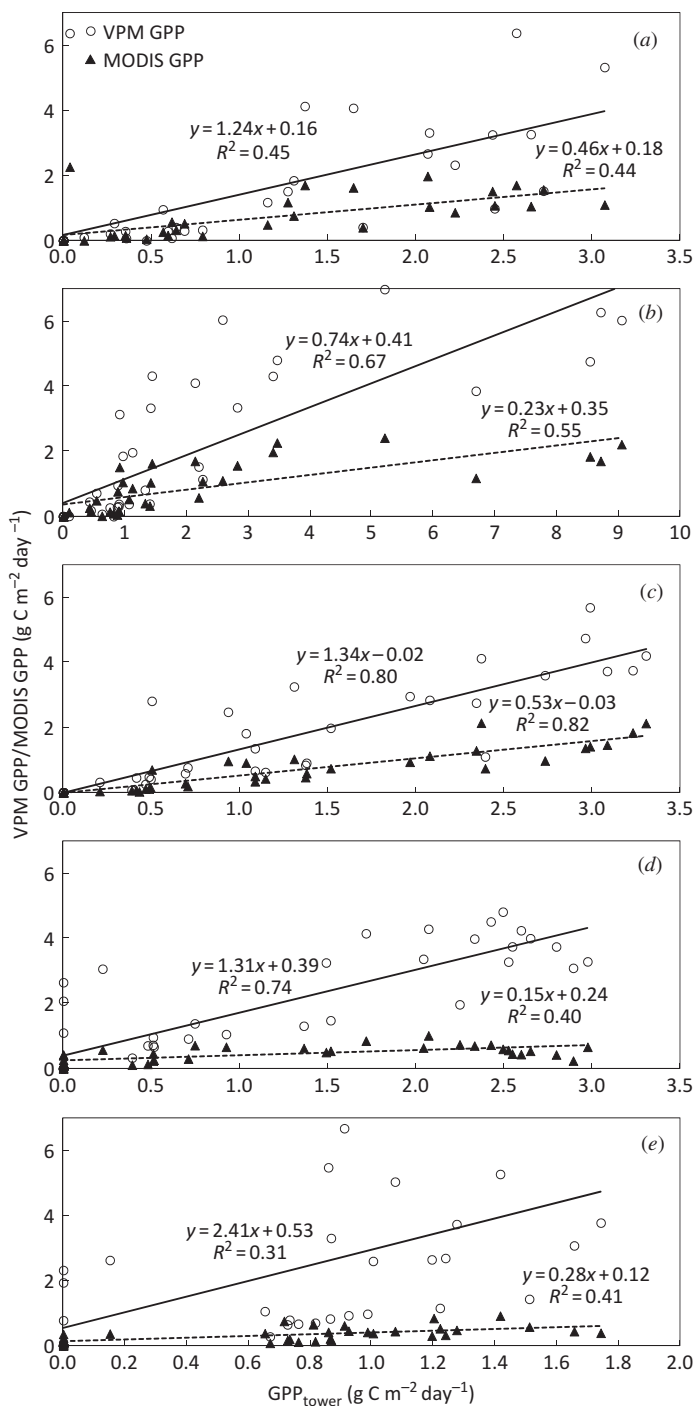
Figure 5. Linear regression of observed GPP$_{tower}$ with predicted GPP$_{VPM}$ and GPP$_{MODIS}$ at five flux sites in 2006: (*a*) Duolun steppe, (*b*) Duolun cropland, (*c*) Xilinhaote steppe, (*d*) Kubuqi poplar plantation, and (*e*) Kubuqi shrubland. The solid line shows regression analysis between GPP$_{tower}$ and GPP$_{VPM}$, while the dashed line is the regression between GPP$_{tower}$ and GPP$_{MODIS}$ product ($p < 0.01$).
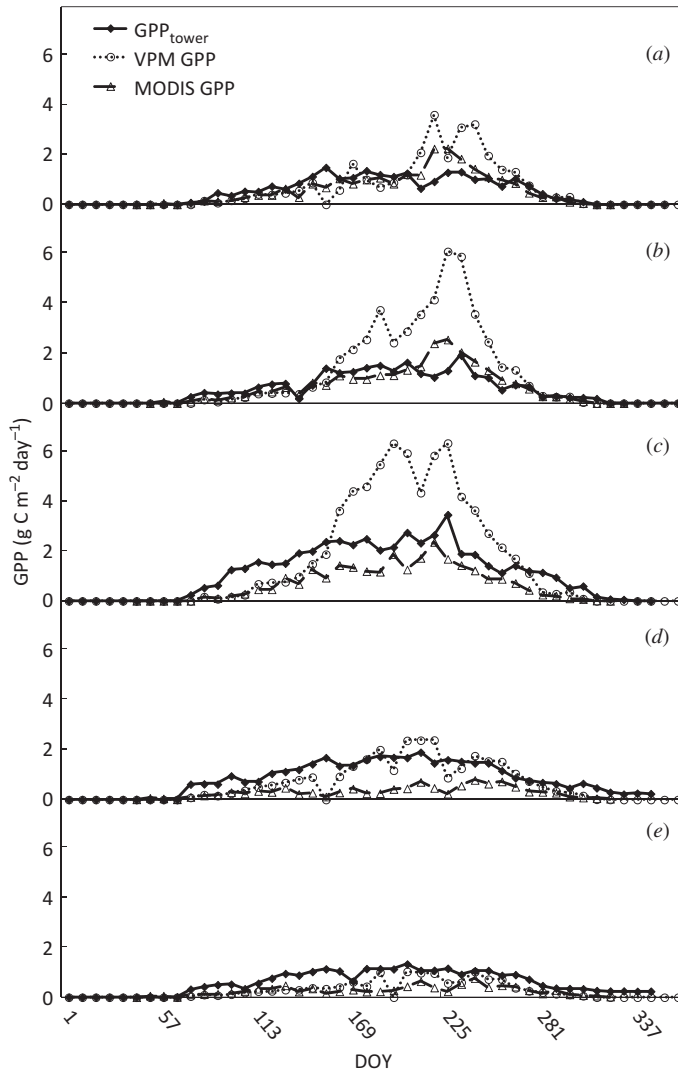
Figure 6.   Seasonal changes in observed GPP$_{tower}$ with predicted GPP$_{VPM}$ and GPP$_{MODIS}$ at five flux sites in 2007: (*a*) Duolun steppe, (*b*) Duolun cropland, (*c*) Xilinhaote steppe, (*d*) Kubuqi poplar plantation, and (*e*) Kubuqi shrubland.

3.3.   *VPM model output and tower GPP*

The VPM model is run on an 8 day time scale with EC tower inputs such as air temperature and summed PAR in conjunction with satellite-derived vegetation indices. The intra-annual dynamics of predicted GPP$_{VPM}$ were compared with the observed GPP$_{tower}$ in 2006 (Figure 4) and 2007 (Figure 6). However, the reduced amplitude in 2007 when compared to 2006 (Figure 3) might be attributed to relatively less precipitation in 2007 (Table 1). The cumulative rainfall in 2006 was almost twice that of 2007 for D01 and D02, 20 mm more in the X03 typical steppe and ~29 mm at the K05 desert steppe sites (Table 1). We reason that the difference in precipitation between 2006 (wet year) and 2007 (dry year)
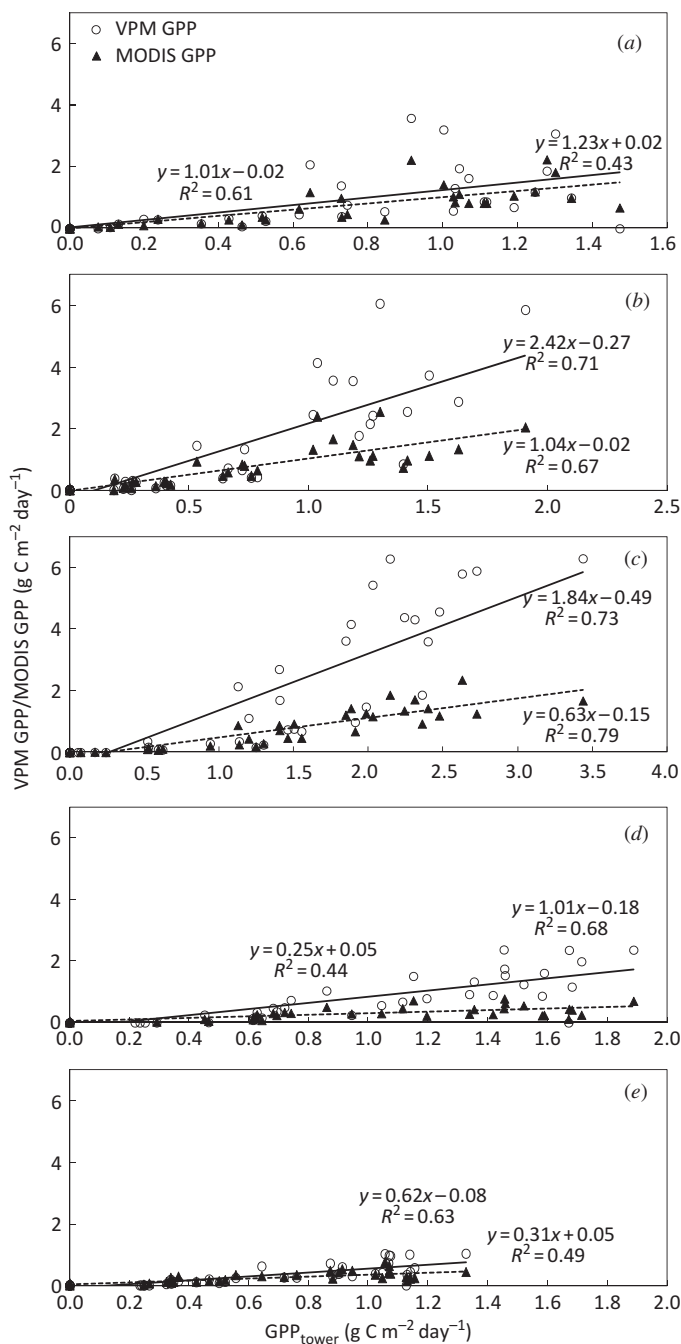
Figure 7. Linear regression of observed GPP_{tower} with predicted GPP_{VPM} and GPP_{MODIS} at five flux sites in 2007: (*a*) Duolun steppe, (*b*) Duolun cropland, (*c*) Xilinhaote steppe, (*d*) Kubuqi poplar plantation, and (*e*) Kubuqi shrubland. The solid line shows regression analysis between GPP_{tower} and GPP_{VPM}, while the dashed line is the regression between GPP_{tower} and GPP_{MODIS} product ($p < 0.01$).

affect the interannual dynamics of LSWI, which is an important driver of the VPM and MVPM models.

A linear regression of GPP$_{VPM}$ with GPP$_{tower}$ as the dependent variable shows reasonable agreement and explains a significant amount of the variation (Table 5, Figures 5 and 6). The results are statistically significant ($p < 0.01$). Modelling efficiency decreased from the X03 site in the typical steppe to the K04 and K05 sites in the desert steppe (Table 4). The GPP$_{VPM}$ at K04 overestimated the GPP$_{tower}$ in 2006, with a PE bias of 28.69 g C m^{-2} year^{-1} and an RMSE of 0.85 g C m^{-2}day^{-1} (Table 5). However, the trend was reversed in 2007 with GPP$_{VPM}$ underestimating the GPP$_{tower}$ with a PE of –10.61 g C m^{-2} year^{-1} and RMSE of 0.42 g C m^{-2}day^{-1} (Table 5). The predicted GPP$_{VPM}$ at the K05 tower sites showed similar statistics and overestimated the observed GPP$_{tower}$ in 2006 (PE = 56.04 g C m^{-2} year^{-1} and RMSE = 2.02 g C m^{-2}day^{-1}) and underestimated GPP$_{tower}$ in 2007 (Tables 4 and 5, Figure 5(*e*)). At X03, the integrated GPP$_{VPM}$ over the active growing season (May–October) and over the entire year was slightly higher than the GPP$_{tower}$ in 2006, with a low bias (Table 5, PE = 9.74 g C m^{-2} year^{-1} and RMSE = 0.72 g C m^{-2}day^{-1}). However, the GPP$_{VPM}$ for both time periods were much higher and overestimated GPP$_{tower}$ in 2007 (Table 4, Figure 7(*c*)) with a PE bias of 20.06 g C m^{-2} year^{-1} and RMSE of 1.10 g C m^{-2}day^{-1} (Table 5). The simulated GPP$_{VPM}$ at the D02 cropland site closely matched GPP$_{tower}$ during the active growing season and the entire year in 2006 (PE = –4.04 g C m^{-2} year^{-1} and RMSE = 1.22 g C m^{-2}day^{-1}), while the GPP$_{VPM}$ overestimated the GPP$_{tower}$ in 2007 with a PE bias of 21.35 g C m^{-2} year^{-1} and RMSE of 0.87 g C m^{-2}day^{-1} (Tables 4 and 5). There was an overestimation of GPP$_{VPM}$ at the D01 typical steppe site during the active growing season as well as the entire year in 2006 (PE = 29.42 g C m^{-2} year^{-1} and RMSE = 1.22 g C m^{-2}day^{-1}), but GPP$_{VPM}$ reasonably matched GPP$_{tower}$ in 2007 (Table 4), with a low bias of RMSE = 0.87 g C m^{-2}day^{-1} (Table 5), partially because of missing/bad data in June and July of 2006 (D0Y = 153 – 209).

In 2006, at D02, X03, and K04, the GPP$_{VPM}$ tracks GPP$_{tower}$ closely, although the magnitudes are not always consistent (Figures 4 and 6). This is especially true for the D02 cropland tower in the peak growing season, where GPP$_{tower}$ is higher than GPP$_{VPM}$. The growing season curve for D02 has a sharp, narrow peak that is characteristic of agriculture with a short growing season. While the seasonal dynamics of GPP in a semi-arid steppe could be explained by temperature and PAR, the cropland land-use type is not a natural ecosystem like the surrounding matrix of semi-arid grassland, even though they both have similar climatic conditions. The seasonal dynamics of D02 can be explained by the cultivation stages of seeding, fertilizer application, and harvesting. With the onset of spring, the GPP$_{VPM}$ in the typical steppe increases gradually, while the cropland site is in dormancy until a rapid increase of D02 GPP$_{VPM}$ in late April/early May (Figure 4(*b*)).

3.4. *MVPM model output and tower GPP*

The observed GPP$_{tower}$ at EC towers was regressed with the simulated GPP$_{MVPM}$ estimate. The regression model showed a strong correlation between GPP$_{tower}$ and GPP$_{MVPM}$ in both the typical steppe site (X03) and irrigated poplar stand (K04) in 2006 and 2007, where the MVPM model performed better than the VPM model (Table 4, Figures 8(*c*) and (*d*)), with a low bias for XO3 (RMSE = 4.78 and 6.06 g C m^{-2}day^{-1} in 2006 and 2007, respectively) and K04 (RMSE = 3.94 and 4.21 g C m^{-2}day^{-1}, respectively) (Table 6). The regression model also explained a significant amount of variation in GPP$_{MVPM}$ for D02 cropland, K05 desert shrubland, and D01 typical steppe in 2007 (Table 6, Figures 8(*b*) and (*e*)). The results were significant ($p < 0.01$), except for D01 in 2006, owing to missing data in the months of
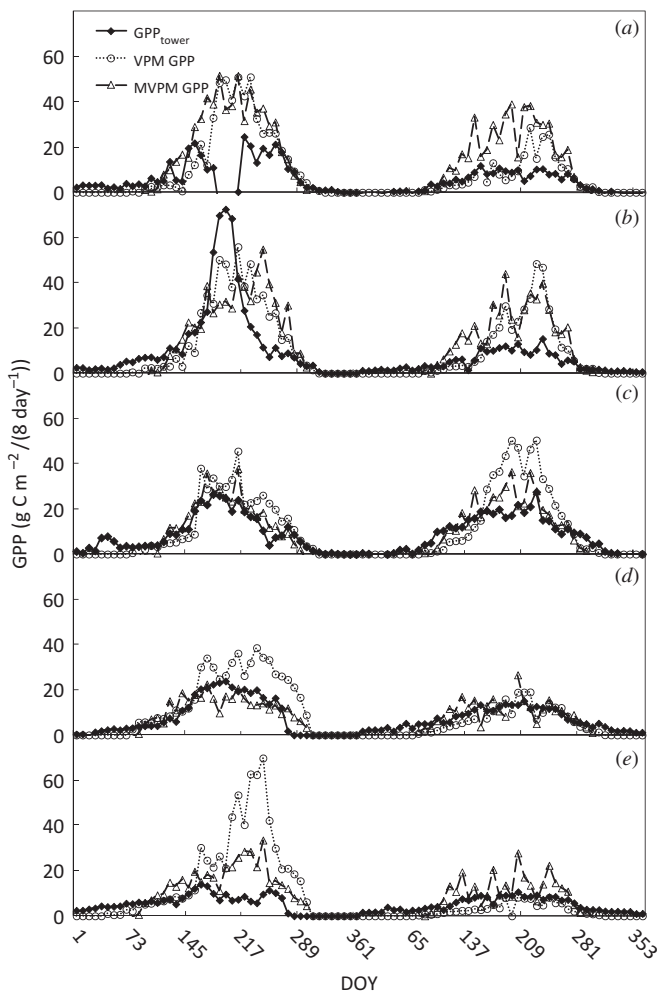
Figure 8. A comparison of the seasonal changes in observed GPP$_{tower}$ with predicted GPP$_{VPM}$ and GPP$_{MVPM}$ at five flux sites in 2006 and 2007: (*a*) Duolun steppe, (*b*) Duolun cropland, (*c*) Xilinhaote steppe, (*d*) Kubuqi poplar plantation, and (*e*) Kubuqi shrubland.

June and July. This also explains the high estimates of GPP$_{MVPM}$ at the D01 typical steppe site (Table 4) with a PE bias of 39.00 and 38.40 g C m^{-2} year^{-1} and RMSE of 17.90 and 9.16 g C m^{-2}day^{-1} in 2006 and 2007, respectively (Table 6). GPP$_{MVPM}$ integrated over the entire year in 2006 at D02 slightly underestimated GPP$_{tower}$, (PE = −2.80 g C m^{-2} year^{-1} and RMSE = 15.28 g C m^{-2}day^{-1}), whereas it was overestimated in the active growing season, especially in 2007 (Tables 4 and 6, RMSE = 7.91 g C m^{-2}day^{-1}). The GPP$_{MVPM}$ at X03 closely matched the integrated GPP$_{tower}$ over the entire year in 2006, with a low PE and RMSE of –0.10 g C m^{-2} year^{-1} and 4.78 g C m^{-2}day^{-1}, respectively (Tables 4 and 6). However, the GPP$_{MVPM}$ overestimated GPP$_{tower}$ in the active growing season in 2007 with a PE bias of 4.37 g C m^{-2} year^{-1} and an RMSE of 6.06 g C m^{-2}day^{-1}. In the desert steppe, at the K04 irrigated poplar stand, GPP$_{MVPM}$ had similar statistics and had a bias in 2006 (PE = −2.80 g C m^{-2} year^{-1} and RMSE = 3.94 g C m^{-2}day^{-1}) and 2007 (PE = –4.80 g C m^{-2} year^{-1} and RMSE = 4.21 g C m^{-2}day^{-1}, Table 6). While the GPP$_{MVPM}$

Table 6. Comparison of model R^2 and RMSE from linear regression and PE of GPP_{MVPM} with GPP_{tower} in five semi-arid LCLU types.

Site	Year	Slope	Significance (p)	R^2	SE	PE	RMSE
DO1	2006	0.049	0.642	0.008*	1.79	39.0	17.96
	2007	0.177	0.001	**0.53**	0.033	38.4	9.16
DO2	2006	0.582	0.014	0.20	1.52	−2.8	15.28
	2007	0.241	0.001	**0.63**	0.035	32.6	7.91
XO3	2006	0.656	0.001	**0.84**	0.540	−0.1	4.78
	2007	0.437	0.001	**0.70**	0.056	4.37	6.06
KO4	2006	1.117	0.001	**0.56**	0.197	−2.8	3.94
	2007	0.410	0.001	**0.47**	0.085	−4.8	4.21
KO5	2006	0.200	0.013	0.20	0.076	22.9	7.48
	2007	0.218	0.001	**0.41**	0.050	10.6	5.64

Notes: *indicates missing data for June–July 2006. Values of R^2 in bold are significant with $p < 0.001$.

overestimated GPP_{tower} at the K05 shrubland site in the annual growing season of 2006 (Table 4, Figure 8(*e*)), it outperformed the VPM in its ability to describe the vegetation dynamics with a lower PE of 22.90 g C m^{-2} year^{-1} in 2006 and in its ability to follow the dynamics of the GPP_{tower} more closely (Tables 5 and 6, Figure 8(*e*)).

4. Discussion

We evaluated the potential of the VPM model to estimate GPP from EC flux towers in different semi-arid LCLU types. In addition, we developed and tested a modified version of the VPM that was validated with tower-derived GPP. Both the VPM and MVPM models have simple structures and few parameters to be adjusted. For example, the VPM model needs just four parameters: temperature, PAR and LUE for each vegetation type, along with vegetation indices (EVI and LSWI) from MODIS in a simple equation, and it is able to reproduce spatiotemporal changes in GPP (Xiao et al. 2005; Li et al. 2007).

When used with ancillary data such as maps of biome, terrestrial ecoregions, land use/land cover (e.g. International Geosphere-Biosphere Programme (IGBP)), meteorological data, satellite-derived albedo, and shortwave radiation, the models provide a good understanding of carbon fluxes with high temporal and spatial resolution that matches the 500 m to 1 km IGBP LCLU MODIS (MOD12Q1) product. Although there are many process-based biogeochemical models (e.g. Simple Biosphere Model 3 (SiB3) and Biome-BGC) that simulate carbon and water fluxes with high temporal resolution (e.g. hourly), they require multiple input parameters that are often difficult to obtain. For example, some SiB2 regional simulation runs need more than 40 spatially interpolated parameters (Wang et al. 2007). The input parameters of process-based models often need frequent recalibration, which is computationally intensive.

The MVPM model offers an alternative to existing PEM-based GPP models in that it is independent of ground-based measurements and entirely based on MODIS data with consistent spatial resolution. The establishment of climate stations or EC flux towers is both expensive and time-consuming, especially in a remote region like the Mongolian Plateau. The MVPM model can help to obtain an estimate of 8 day GPP from the previous year before setting up an EC flux tower site in a semi-arid region.

Similar models based solely on MODIS EVI also exist (Sims et al. 2006b). However, Sims et al. (2006b) found poor GPP estimates in the active season for sites undergoing

drought as their model lacked measures of drought stress and temperature, which are present in the MOD17 GPP model (Running et al. 2004). The MODIS LST product (MOD11A2), which is a measure of 'skin' temperature when compared to air temperature, normally measured by meteorological stations, is also well correlated with VPD (Wan et al. 2004; Jin et al. 2010). We optimized the MVPM model for GPP in semi-arid regions by including LST and LSWI to account for variability in temperature and vegetation water content as well as drought stress, which are the key regulators of carbon fluxes in dryland regions. This may be an improvement over the VPM model, where the absence of a soil moisture component and its inability to measure water stress might be a source of error.

The advance of the growing season, or phenological cycle (leaf flush/green-up, maturity, senescence, and dormancy), is characterized by biochemical changes in the vegetation canopy (e.g. chlorophyll, xanthophyll), which, in turn, affect the biophysical properties of the semi-arid land surface such as evapotranspiration, albedo, and surface roughness (Xiao et al. 2004a, 2004b). Huete et al. (2002) described the biophysical/radiometric advantages and relative merits of EVI and NDVI, especially in sparsely vegetated environments with pronounced soil background signature. This study evaluates the use of productivity and water indices such as EVI and LSWI to measure the growing season length and water stress that regulate carbon exchange in the ecosystem. The predicted GPP_{VPM} agrees well with observed GPP_{tower} in the semi-arid ecosystem types in Inner Mongolia. Our results suggest that EVI can be linearly related to fPAR and chlorophyll, while LSWI seems to be a reasonable surrogate of leaf water content as was found in VPM studies in various forest ecosystems (Xiao et al. 2004a, 2004b, 2005). The MVPM and VPM models provide an alternate to the MODIS GPP product (Running et al. 2004), which is based on the NDVI – fPAR – LAI relationship. GPP_{MODIS} depends a great deal upon the availability and quality of daily meteorological observation data from NASA's DAO **(**Zhao, Running, and Nemani 2006**)**. Previous studies showed that VPD could capture the interannual variability of the water stress in wet areas where the annual precipitation was >400 mm year^{-1}. However, in arid regions where soil moisture is the limiting factor, MOD17 was found to underestimate water stress and overestimate GPP. It was found that MOD17 was better able to describe the intraannual and interannual variability of GPP in the lower 48 states of the USA than in monsoon-controlled China (Mu et al. 2007b).

Extensive validation of the MODIS GPP product was carried out by the BIGFOOT project, which involved the use of traditional ecological measurements as well as process-based modelling through the use of Biome-BGC (Turner et al. 2005). While MODIS GPP could successfully track the seasonality of site GPP across different climatic regimes that include temperate deciduous and evergreen forests, alpine forests, wet and dry savanna, and so on (Running et al. 2004), it failed in accurately estimating the magnitude of GPP in water-limited ecosystems (Leuning et al. 2005; Zhang et al. 2007). The validation sites include a single desert grassland site (Sevilleta Long Term Ecological Research Site (SEVI)) where the MODIS GPP product did not agree well with the tower GPP, especially in the beginning and at the end of the growing season (Turner et al. 2005). This suggests the need for more GPP product validation in semi-arid grasslands as opposed to most validation studies, which take place in various forest ecosystems.

The GPP_{VPM} and GPP_{MVPM} differ from the GPP_{tower} observations in some 8 day periods (Figures 4, 6, and 8), and these account for the differences between the annual and active growing season integration of predicted and observed GPP (Table 3). These differences can be attributed to the sensitivity of the model towards microclimatic variations in PAR and temperature, which vary among the five LCLU types. Schwalm et al. (2010) found that model performance in predicting NEE was better at forest sites when compared

to grassland and forest sites. Another source of error could stem from the overestimation or underestimation of GPP by the EC towers. In order to calculate GPP, ecosystem respiration has to be measured in addition to the gap filling of NEE measured by the tower. These steps are subjective and are potential sources of error leading to uncertainty (Falge et al. 2001, 2002). In spite of its limitations, the EC method has the potential to accurately measure LUE across semi-arid ecosystems as the network of EC towers increases globally. A possible source of error leading to the overestimation of GPP_{VPM} and GPP_{MVPM} is the use of 8 day surface reflectance (M0D09A1V005), which has no bidirectional reflectance distribution function (BRDF) correction or normalization, resulting in the derived spectral indices being affected by angular geometry and extreme look angles (Li et al. 2007). Similarly, Collection 5 MODIS products could contribute to the modelling error by overestimation of LST and fPAR, especially over bare soil surfaces in semi-arid regions. Although the maximum MODIS fPAR might be close to *in situ* observations in the peak growing season, the opposite might be true for semi-arid areas with sparse vegetation which complicates radiative transfer modelling, resulting in overestimation at sites where values of fPAR are low (Turner et al. 2006).

The difference in amplitude between the two growing seasons could be attributed to variable rainfall as can be expected in a water-limited ecosystem. Miao et al. (2009) found that precipitation at Duolun sites in 2006 was higher than the 11 year average, while the 2007 growing season experienced below-average rainfall. Precipitation at Xilinhaote was below the long-term mean, with the growing seasons of 2006 and 2007 being abnormally dry years. The lagged peak in the growing season was confirmed by an independent study with D01, D02, and X03, reaching peak values in July of 2006 when compared to August of 2007 growing season (Miao et al. 2009). In addition, integrated GPP_{tower} values for the 2007 growing season were significantly lower at D01 and D02 when compared to the 2006 season, with similar results reported by Miao et al. (2009).

Finally, GPP measurements might be higher than expected in arid and semi-arid regions due to an increase in irrigated agriculture, even though evapotranspiration exceeds precipitation (Mu et al. 2007a), which is ∼150 mm annually (Kang et al. 2007). This is especially true along the desert margin in Inner Mongolia, where the typical steppe gives way to desert steppe (e.g. the Hetao irrigation district along the Yellow River; John et al. 2009). Higher-than-expected evapotranspiration measurements in the desert steppe can also be attributed to subsurface flow and water infiltration within the Huang He (Yellow River) basin (Feng, Wang, and Feng 2005; Wilske et al. 2009).

5. Conclusion

We used carbon flux data obtained from EC towers at five sites in semi-arid Inner Mongolia to validate the intraannual dynamics of GPP using the VPM and MVPM models in conjunction with microclimatic variables such as PAR and air temperature. Although the VPM needs just four parameters obtained from flux towers for each of the five ecosystem LCLU types, the MVPM is independent of any ground-measured meteorological data. Both models are based on simple equations that are not computationally intensive, like most process-based models. The MVPM model, in particular, offers a cost-effective solution for predicting GPP at remote study sites that lack the infrastructure to set up ground-based sensors. Our results indicate a reasonable agreement between the observed GPP_{tower} and the predicted GPP_{VPM} and GPP_{MVPM}, indicating the potential for these satellite-driven models to predict GPP in semi-arid ecosystems. However, different sources of error, either from the flux tower measurements or MODIS-derived indices/products, introduced uncertainties

that led to the overestimation of GPP by the VPM and MVPM models. In addition, environmental factors such as precipitation and ground water flow as well as landscapes with a high degree of anthropogenic modification (e.g. croplands and irrigated poplar stands) play a role in a phase shift in predicted GPP when compared to GPP observed at EC towers. The ability to model *in situ* temporal measurements of carbon fluxes to the region is the first step to obtain a better understanding of the carbon cycle in semi-arid Inner Mongolia and might enable the estimation and modelling of evapotranspiration and water-use efficiency in future studies.

References

Aalto, T., P. Ciais, and A. Chevillard. 2004. "Optimal Determination of the Parameters Controlling Biospheric CO_2 Fluxes over Europe Using Eddy Covariance Fluxes and Satellite NDVI Measurements." *Tellus* 56B: 93–104.

Aber, J. D. 1997. "Why Don't We Believe the Models?" *Bulletin of the Ecological Society of America* 78: 232–3.

Baldocchi, D. D., E. Falge, L. Gu, R. Olson, D. Hollinger, S. Running, P. Anthoni, C. Bernhofer, K. Davis, J. Fuentes, A. Goldstein, G. Katul, B. Law, X. Lee, Y. Malhi, T. Meyers, J. W. Munger, W. Oechel, K. Pilegaard, H. P. Schmid, R. Valentini, S. Verma, T. Vesala, K. Wilson, and S. Wofsy. 2001. "FLUXNET: A New Tool to Study the Temporal and Spatial Variability of Ecosystem-Scale Carbon Dioxide, Water Vapor and Energy Flux Densities." *Bulletin of the American Meteorological Society* 82: 2415–35.

Burba, G. G., D. K. McDermitt, A. Grelle, D. J. Anderson, and L. Xu. 2008. "Addressing the Influence of Instrument Surface Heat Exchange on the Measurements of CO_2 Flux from Open-Path Gas Analyzers." *Global Change Biology* 14: 1854–76.

Chase, T. N., R. A. Pielke, J. Knaff, T. Kittel, and J. Eastman. 2000. "A Comparison of Regional Trends in 1979–1997 Depth-Averaged Tropospheric Temperatures." *International Journal of Climatology* 20: 503–18.

Chen, S., J. Chen, G. Lin, W. Zhang, H. Miao, L. Wei, J. Huang, and X. Han. 2009. "Energy Balance and Partition in Inner Mongolia Steppe Ecosystems with Different Land Use Types." *Agricultural Forest Meteorology* 149: 1800–9.

Christensen, L., M. B. Coughenour, J. E. Ellis, and Z. Z. Chen. 2004. "Vulnerability of the Asian Typical Steppe to Grazing and Climate Change." *Climatic Change* 63: 351–68.

Falge, E., D. Baldocchi, R. J. Olson, P. Anthoni, M. Aubinet, C. Bernhofer, G. Burba, R. Ceulemans, R. Clement, H. Dolman, A. Granier, P. Gross, T. Grünwald, D. Hollinger, N.-O. Jensen, G. Katul, P. Keronen, A. Kowalski, C. Ta Lai, B. E. Law, T. Meyers, J. Moncrieff, E. Moors, J. W. Munger, K. Pilegaard, Ü. Rannik, C. Rebmann, A. Suyker, J. Tenhunen, K. Tu, S. Verma, T. Vesala, K. Wilson, and S. Wofsy. 2001. "Gap Filling Strategies for Longterm Energy Flux Data Sets." *Agricultural Forest Meteorology* 107: 71–7.

Falge, E., D. Baldocchi, J. Tenhunen, M. Aubinet, P. Bakwin, P. Berbigier, C. Bernhofer, G. Burba, R. Clement, K. J. Davis, J. A. Elbers, A. H. Goldstein, A. Grelle, A. Granier, J. Guðmundsson, D. Hollinger, A. S. Kowalksi, G. Katul, B. E. Law, Y. Malhi, T. Meyers, R. K. Monson, J. W. Munger, W. Oechel, K. T. Paw, K. Pilegaard, Ü. Raanik, C. Rebemann, A. Suker, R. Valentinni, K. Wilson, and S. Wofsy. 2002. "Seasonality of Ecosystem Respiration and Gross Primary Production as Derived from FLUXNET Measurements." *Agricultural Forest Meteorology* 113: 53–74.

Feng, Z. Z., X. K. Wang, and Z. W. Feng. 2005. "Soil N and Salinity Leaching after the Autumn Irrigation and Its Impact on Groundwater in Hetao Irrigation District, China." *Agricultural Water Management* 71: 131–43.

Fensholt, R., I. Sandholt, and S. Rasmussen. 2004. "Evaluation of MODIS LAI, fAPAR and the Relation between fAPAR and NDVI in a Semi-Arid Environment Using In Situ Measurements." *Remote Sensing of Environment* 91: 490–507.

Foken, T., and B. Wichura. 1996. "Tools for Quality Assessment of Surface-Based Flux Measurements." *Agricultural Forest Meteorology* 78: 83–105.

Gitelson, A. A. 2004. "Wide Dynamic Range Vegetation Index for Remote Quantification of Biophysical Characteristics of Vegetation." *Journal of Plant Physiology* 161: 165–73.

Goetz, S. J., S. D. Prince, S. N. Goward, M. M. Thawley, and J. Small. 1999. "Satellite Remote Sensing of Primary Production: An Improved Production Efficiency Modeling Approach." *Ecoogical Modelling* 122: 239–55.

Goward, S. N., C. J. Tucker, and D. G. Dye. 1985. "North American Vegetation Patterns Observed with the NOAA-7 Advanced Very High Resolution Radiometer." *Vegetation* 64: 3–14.

Hu, Z. Z., S. Yang, and R. Wu. 2003. "Long-Term Climate Variations in China and Global Warming Signals." *Journal of Geophysical Research* 108: 4614.

Huete, A., K. Didan, T. Miura, and E. Rodriguez. 2002. "Overview of the Radiometric and Biophysical Performance of the MODIS Vegetation Indices." *Remote Sensing of Environment* 83: 195–213.

IPCC. 2007. "Summary for Policy Makers." In *Climate Change 2007: Impacts, Adaptation and Vulnerability. Contribution of Working Group II to the Fourth Assessment Report of the Inter Governmental Panel on Climate Change (IPCC)*, edited by M. L. Parry, O. F. Canziani, J. P. Palutikof, P. J. van der Linden and C. E. Hanson, 7–22. Cambridge: Cambridge University Press.

Jin, M. L., and R. E. Dickinson. 2010. "Land Surface Skin Temperature Climatology: Benefitting from the Strengths of Satellite Observations." *Environmental Research Letters* 5: 44004. doi:10.1088/1748-9326/5/4/044004.

John, R., J. Chen, N. Lu, and B. Wilske. 2009. "Land Cover/Land Use Change in Semi-Arid Inner Mongolia: 1992–2004." *Environmental Research Letters* 4: 045010. doi:10.1088/1748–9326/4/4/045010.

Jung, M., M. Reichstein, P. Cias, S. I. Seneviratne, J. Sheffield, M. L. Goulden, G. Bonan, A. Cescatti, J. Chen, R. de Jeu, A. J. Dolman, W. Eugster, D. Gerten, D. Gianelle, N. Gobron, J. Heinke, J. Kimball, B. E. Law, L. Montagnani, Q. Mu, B. Mueller, K. Oleson, D. Papale, A. Richardson, O. Roupsard, S. Running, E. Tomelleri, N. Viovy, U. Weber, C. Williams, E. Wood, S. Zaehle, and K. Zhang. 2010. "Recent Decline in the Global Land Evapotranspiration Trend Due to Limited Moisture Supply." *Nature* 467: 951–54.

Kang, L., X. Han, Z. Zhang, and O. J. Sun. 2007. "Grassland Ecosystems in China: Review of Current Knowledge and Research Advancement." *Philosophical Transactions of the Royal Society* 362: 997–1008. doi:10.1098/rstb.2007.2029.

Kanniah, K. D., J. Beringer, N. J. Tapper, L. B. Hutley, and X. Zhu. 2009. "Evaluation of Collections 4 and 5 of the MODIS Gross Primary Productivity Product and Algorithm Improvement at a Tropical Savanna Site in Northern Australia." *Remote Sensing of Environment* 113: 1808–22.

Leuning, R., H. A. Cleugh, S. J. Zegelin, and D. Hughes. 2005. "Carbon and Water Fluxes over a Temperate Eucalyptus Forest and a Tropical Wet/Dry Savanna in Australia: Measurements and Comparison with MODIS Remote Sensing Estimates." *Agricultural and Forest Meteorology* 129: 151–73.

Li, S., Y. Harazono, T. Oikawa, H. Zhao, Z. He, and X. Chang. 2000. "Grassland Desertification by Grazing and the Resulting Micrometeorological Changes in Inner Mongolia." *Agricultural Forest Meteorology* 102: 125–37.

Li, Z., G. Yu, X. Xiao, Y. Li, X. Zhao, C. Ren, L. Zhang, and Y. Fu. 2007. "Modeling Gross Primary Production of Alpine Ecosystems in the Tibetan Plateau Using MODIS Images and Climate Data." *Remote Sensing of Environment* 107: 510–19.

Lu, N., B. Wilske, J. Ni, R. John, and J. Chen 2009. "Climate Change in Inner Mongolia from 1955–2005 – Trends at Regional, Biome and Local Scales." *Environmental Research Letters* 4: 045006. doi: 10.1088/1748-9326/4/4/045006.

McCree, K. J. 1972. "Test of Current Definitions of Photosynthetically Active Radiation against Actual Leaf Photosynthesis Data." *Agricultural Meteorology* 10: 443–53.

Miao, H., S. Chen, J. Chen, W. Zhang, P. Zhang, L. Wei, X. Han, and G. Lin 2009. "Cultivation and Grazing Altered Evapotranspiration and Dynamics in Inner Mongolia Steppes." *Agricultural and Forest Meteorology* 149: 1810–19.

Moffat, A. M., D. Papale, M. Reichstein, D. Y. Hollinger, A. D. Richardson, A. G. Barr, C. Beckstein, B. H. Braswell, G. Churkina, A. R. Desai, E. Falge, J. H. Gove, M. Heimann, D. Hui, A. J. Jarvis, J. Kattge, A. Noormets, and V. J. Stauch. 2007. "Comprehensive Comparison of Gap Filling Techniques for Eddy Covariance Net Carbon Fluxes." *Agricultural Forest Meteorology* 147: 209–32.

Monteith, J. L. 1972. "Solar Radiation and Productivity in Tropical Ecosystems." *Journal of Applied Ecology* 9: 747–66.

Mu, Q., F. A. Heinsch, M. Zhao, and S. W. Running. 2007a. "Development of a Global Evapotranspiration Algorithm Based on MODIS and Global Meteorology Data." *Remote Sensing of Environment* 111: 519–36.

Mu, Q., M. Zhao, F. A. Heinsch, M. Liu, H. Tian, and S. W. Running. 2007b. "Evaluating Water Stress Controls on Primary Production in Biogeochemical and Remote Sensing Based Models." *Journal of Geophysical Research* 112: G01012. doi: 10.1029/2006JG000179.

Noormets, A., J. Chen, and T. R. Crow. 2007. "Age-Dependent Changes in Ecosystem Carbon Fluxes in Managed Forests in Northern Wisconsin." *USA Ecosystems* 10: 187–203.

Ojima, D. S., X. Xiao, T. Chuluun, and X. S. Zhang. 1998. "Asian Grassland Biogeochemistry: Factors Affecting Past and Future Dynamics of Asian Grasslands." In *Asian Change in the Context of Global Climate Change: Impact of Natural and Anthropogenic Changes in Asia on Global Biogeochemistry*, edited by J. Galloway and J. M. Melillo, 128–44. Cambridge: Cambridge University Press, IGBP Book Series 3.

Osmond, B., G. Ananyev, J. Berry, C. Langdon, Z. Kolber, G. Lin, R. Monson, C. Nichol, U. Rascher, U. Schurr, S. Smith, and D. Yakir. 2004. "Changing the Way We Think about Global Change Research: Scaling up in Experimental Ecosystem Science." *Global Change Biology* 10: 393–407.

Parton, W. J., J. M. O. Scurlock, D. S. Ojima, D. S. Schimel, and D. O. Hall. 1995. "Impact of Climate Change on Grassland Production and Soil Carbon Worldwide." *Global Change Biology* 1: 13–22.

Raich, J. W., E. B. Rastetter, J. M. Melillo, D. W. Kicklighter, P. A. Steudler, B. J. Peterson, A. L. Grace, B. Moore III, and C. J. Vorosmarty. 1991. "Potential Net Primary Productivity in South America—Application of a Global Model." *Ecological Applications* 1: 399–429.

Ruimy, A., L. Kergoat, and A. Bondeau. 1999. "Comparing Global Models of Terrestrial Net Primary Productivity (NPP): Analysis of Differences in Light Absorption and Light-Use Efficiency." *Global Change Biology* 5: 56–64.

Ruimy, A., B. Saugier, and G. Dedieu. 1994. "Methodology for the Estimation of Terrestrial Net Primary Production from Remotely Sensed Data." *Journal of Geophysical Research* 99: 5263–84.

Running, S. W., D. D. Baldocchi, D. P. Turner, S. T. Gower, P. S. Bakwin, and A. Hibbard. 1999. "A Global Terrestrial Monitoring Network Integrating Tower Fluxes, Flask Sampling, Ecosystem Modeling, and EOS Satellite Data." *Remote Sensing of Environment* 70: 108–27.

Running, S. W., R. R. Nemani, F. A. Heinsch, M. Zhao, M. Reeves, and H. Hashimoto. 2004. "A Continuous Satellite-Derived Measure of Global Terrestrial Primary Production." *BioScience* 54: 547–60.

Schotanus, P., F. T. M. Nieuwstadt, and H. A. R. De Bruin. 1983. "Temperature Measurement with a Sonic Anemometer and Its Application to Heat and Moisture Fluxes." *Boundary-Layer Meteorology* 26: 81–93.

Schwalm, C. R., C. A. Williams, K. Schaefer, R. Anderson, M. A. Arain, I. Baker, A. Barr, T. A. Black, G. Chen, J. M. Chen, P. Ciais, K. J. Davis, A. Desai, M. Dietze, D. Dragoni, M. L. Fischer, L. B. Flanagan, R. Grant, L. Gu, D. Hollinger, R. C. Izaurralde, C. Kucharik, P. Lafleur, B. E. Law, L. Li, Z. Li, S. Liu, E. Lokupitiya, Y. Luo, S. Ma, H. Margolis, H. Mccaughey, R. K. Monson, W. C. Oechel, C. Peng, B. Poulter, D. T. Price, D. M. Riciutto, W. Riley, A. K. Sahoo, M. Sprintsin, J. Sun, H. Tian, C. Tonitto, H. Verbeeck, and S. B. Verma. 2010. "A Model Data Intercomparison of CO$_2$ Exchange across North America: Results from the North American Carbon Program Site Synthesis." *Journal of Geophysical Research* 115: G00H05. doi:10.1029/2009JG001229.

Shabanov, N. V., D. Huang, Y. Knjazikhin, R. E. Dickinson, and R. B. Myneni. 2007. "Stochastic Radiative Transfer Model for Mixture of Discontinuous Vegetation Canopies." *Journal of Quantitative Spectroscopy & Radiative Transfer* 107: 236–62.

Sims, D. A., H. Luo, S. Hastings, W. C. Oechel, A. F. Rahman, and J. A. Gamon. 2006a. "Parallel Adjustments in Vegetation Greenness and Ecosystem CO$_2$ Exchange in Response to Drought in a Southern California Chaparral Ecosystem." *Remote Sensing of Environment* 103: 289–303.

Sims, D. A., A. F. Rahman, V. D. Cordova, B. Z. El-Masri, D. D. Baldocchi, P. V. Bolstad, L. B. Flanagan, A. H. Goldstein, D. Y. Hollinger, L. Misson, R. K. Monson, W. C. Oechel, H. P. Schmid, S. C. Wofsy, and L. Xu. 2008. "A New Model of Gross Primary Productivity for North American Ecosystems Based Solely on the Enhanced Vegetation Index and Land Surface Temperature from MODIS." *Remote Sensing of Environment* 112: 1633–46.

Sims, D. A., A. F. Rahman, V. D. Cordova, B. Z. El-Masri, D. D. Baldochhi, L. B. Flanagan, A. H. Goldstein, D. Y. Hollinger, L. Misson, R. K. Monson, W. C. Oechel, H. P. Schmid, S. C. Wofsy, and L. Xu. 2006b. "On the Use of MODIS EVI to Assess Gross Primary Productivity of North American Ecosystems." *Journal of Geophysical Research* 111: G04015. doi: 10.1029/2006JG000162.

Tucker, C. J. 1979. "Red and Photographic Infrared Linear Combinations for Monitoring Vegetation." *Remote Sensing of Environment* 8: 127–50.

Turner, D. P., W. D. Ritts, W. B. Cohen, S. T. Gower, S. W. Running, M. Zhao, M. H. Costa, A. A. Kisrschbaum, J. M. Ham, S. R. Saleska, and D. E. Ahl. 2006. "Evaluation of MODIS NPP and GPP Products across Multiple Biomes." *Remote Sensing of Environment* 102: 282–92.

Turner, D. P., W. D. Ritts, W. B. Cohen, T. K. Maeirsperger, S. Gower, A. Kirschbaum, S. W. Running, M. Zhao, S. C. Wofsy, A. L. Dunn, B. E. Law, J. C. Campbell, W. C. Oechel, H. J. Kwon, T. P. Meyers, E. E. Small, S. A. Kurc, and J. A. Gamon. 2005. "Site-Level Evaluation of Satellite-Based Global Terrestrial Gross Primary Production and Net Primary Production Monitoring." *Global Change Biology* 11: 666–84.

Vermote, E. F., N. Z. El Saleous, and C. O. Justice. 2002. "Atmospheric Correction of MODIS Data in the Visible to Middle-Infrared First Results." *Remote Sensing of Environment* 83: 1–2, 97–111.

Vermote, E. F., and S. Kotchenova. 2008. "Atmospheric Correction for the Monitoring of Land Surfaces." *Journal of Geophysical Research* 113: D23S90. doi: 10.1029/2007JD009662.

Wan, Z. 2008. "New Refinements and Validation of the MODIS Land-Surface Temperature/Emissivity Products." *Remote Sensing of Environment* 112: 59–74.

Wan, Z., Y. Zhang, and Z.-L. Li. 2002. "Validation of the Land-Surface Temperature Products Retrieved from Terra Moderate Resolution Imaging Spectroradiometer Data." *Remote Sensing of Environment* 83: 163–80.

Wan, Z., Y. Zhang, Q. Zhang, and Z. L. Li. 2004. "Quality Assessment and Validation of the MODIS Global Land Surface Temperature." *International Journal of Remote Sensing* 25: 261–74.

Wang, J. W., A. S. Denning, L. X. Lu, I. T. Baker, K. D. Corbin, and K. J. Davis. 2007. "Observations and Simulations of Synoptic, Regional, and Local Variations in Atmospheric CO_2." *Journal of Geophysical Research* 112: D04108. doi: 10.1029/2006JD007410.

Webb, E. K., G. I. Pearman, and R. Leuning. 1980. "Correction of Flux Measurements for Density Effects Due To Heat and Water Vapor Transfer." *Quarterly Journal of the Royal Meteorological Society* 106: 85–106.

Wilczak, J. M., S. P. Oncley, and S. A. Stage. 2001. "Sonic Anemometer Tilt Correction Algorithms." *Boundary-Layer Meteorology* 99: 127–50.

Wilske, B., N. Lu, L. Wei, S. Chen, T. Zha, C. Liu, W. Xu, A. Noormets, J. Huang, Y. Wei, J. Chen, Z. Zhang, J. Ni, G. Sun, K. Guo, S. Mcnulty, R. John, X. Han, G. Lin, and J. Chen. 2009. "Poplar Plantation Alters Water Balance in Semiarid Inner Mongolia." *Journal of Environmental Management* 90: 2762–70.

Wylie, B. K., D. A. Johnson, E. Laca, N. Z. Saliendra, G. Gilmanov, B. C. Reed, L. Tieszen, and B. Worstell. 2003. "Calibration of Remotely Sensed, Coarse Resolution NDVI to CO_2 Fluxes in a Sagebrush Steppe Ecosystem." *Remote Sensing of Environment* 85: 243–55.

Xiao, X., D. Hollinger, J. D. Aber, M. Goltz, E. A. Davidson, and Q. Zhang. 2004a. "Satellite-Based Modeling of Gross Primary Production in an Evergreen Needle Leaf Forest." *Remote Sensing of Environment* 89: 519–34.

Xiao, X., Q. Zhang, B. Braswell, S. Urbanski, S. Boles, S. C. Wofsy, B. Moore, and D. Ojima. 2004b. "Modeling Gross Primary Production of Temperate Deciduous Broadleaf Forest Using Satellite Images and Climate Data." *Remote Sensing of Environment* 91: 256–70.

Xiao, X., Q. Zhang, S. Saleska, L. Hutyra, P. D. Camargo, S. C. Wofsy, S. Frolking, S. Boles, M. Keller, and B. Moore. 2005. "Satellite-Based Modeling of Gross Primary Production in a Seasonally Moist Tropical Evergreen Forest." *Remote Sensing of Environment* 94: 105–22.

Xiao, J., Q. Zhuang, B. E. Law, D. D. Baldocchi, J. Chen, A. D. Richardson, J. M. Melillo, K. J. Davis, D. Y. Hollinger, S. Wharton, R. Oren, A. Noormets, M. L. Fischer, S. B. Verma, D. R. Cook, G. Sun, S. Mcnulty, S. C. Wofsy, P. V. Bolstad, S. P. Burns, P. S. Curtis, B. G. Drake, M. Falk, D.

R. Foster, L. Gu, J. L. Hadley, G. G. Katul, M. Litvak, S. Ma, T. A. Martin, R. Matamala, T. P. Meyers, R. K. Monson, J. W. Munger, W. C. Oechel, U. K. T. Paw, H. P. Schmid, R. L. Scott, G. Starr, A. E. Suyker, and M. S. Torn. 2011. "Assessing Net Ecosystem Carbon Exchange of U.S. Terrestrial Ecosystems by Integrating Eddy Covariance Flux Measurements and Satellite Observations." *Agricultural Forest Meteorology* 151: 60–9.

Zhai, P., and X. Pan 2003. "Trends in Temperature Extremes during 1951–1999 in China." *Geophysical Research Letters 30*, 1913. doi: 10.1029/2003GL018004.

Zhai, P., A. Sun, F. Ren, X. Liu, B. Gao, and Q. Zhang. 1999. "Changes of Climate Extremes in China." *Climatic Change* 42: 203–18.

Zhang, L., B. Wylie, T. Loveland, E. Fosnight, L. L. Tieszen, and T. Gilmanov. 2007. "Evaluation and Comparison of Gross Primary Production Estimates for the Northern Great Plains Grasslands." *Remote Sensing of Environment* 106: 173–89.

Zhao, M., F. A. Heinsch, R. R. Nemani, and S. W. Running. 2005. "Improvements of the MODIS Terrestrial Gross and Net Primary Production Global Dataset." *Remote Sensing of Environment* 95: 164–76.

Zhao, M., S. W. Running, and R. R. Nemani. 2006. "Sensitivity of Moderate Resolution Imaging Spectroradiometer (MODIS) Terrestrial Primary Production to the Accuracy of Meteorological Reanalyses." *Journal of Geophysical Research* 111: G01002. doi:10.1029/2004JG000004.

Zhou, G., Y. Wang, and S. Wang. 2002. "Responses of Grassland Ecosystems to Precipitation and Land Use Along the Northeast China Transect." *Journal of Vegetation Science* 13: 361–8.